CHAPTER TWELVE

Deep-Sea Corals: New Insights to Paleoceanography

Owen A. Sherwood* *and* Michael J. Risk

Contents

1. Introduction

Deep-sea corals were first described from the coast of Norway, and the first species identified by Linnaeus (1758). Since then, at least until recently, interest in the group has waxed and waned, seemingly in concert with the frequency of their relationship with fishing efforts on the continental shelves.

In recent years, two critical concerns have heightened interest in deep-sea corals. Worldwide decline of coastal fisheries, especially off the shelves on eastern North America, has prompted a re-examination of the role of deep-sea corals as habitat for fishes. In addition, concern about the rate and scale of climate change

* Corresponding author.

Developments in Marine Geology, Volume 1
ISSN 1572-5480, DOI 10.1016/S1572-5480(07)01017-2

has combined with the growing realization that this process can be measured by using the records encoded in coral skeletons. Instrumental records are not sufficiently widespread or long-standing to allow predictive models to be constructed, and proxy records have to be consulted. Other than deep-sea corals, few archives offer the combination of global distribution (Figure 1), temporal resolution, and duration of record. In this chapter, when we speak of deep-sea "corals," we are referring not only to the true corals, the Scleractinia (which date from the Triassic) but any coelenterate that makes a hard skeleton capable of recording climate data (Figure 2). This would include several orders that secrete a horny skeleton, such as Octocorals, (Ordovician-recent), Antipatharians (Miocene-recent) and Zoanthids (recent).

1.1. Overview of Past Work on Geochemistry of Deep-Sea Corals

Previous attempts several decades ago to decipher the climate record in deep-sea corals from stable isotope analyses were overshadowed by the upsurge in interest in records from shallow-water reef corals. Weber (1973) found that deep-sea corals were generally less depleted in $\delta^{18}O$ and $\delta^{13}C$ than were reef corals; Emiliani, Hudson, Shinn, George, and Lidz (1978) described a series of analyses of subsamples of corals from the Blake Plateau, off Florida, and found a progressive up-polyp closer approach to equilibrium values.

Since the early 1970s, paleoceanographic studies have relied heavily on cores from reef corals. Two examples, from hundreds of papers, involve our understanding of El Niño-Southern Oscillation (ENSO) events. Carriquiry and Risk (1988) were the first to establish the record of the timing and intensity of such an event, working up the stable isotopic record in reef corals from the west coast of Costa Rica. Tudhope et al. (2001) analyzed cores from the superbly-exposed and preserved reef terraces of Papua New Guinea, and found that ENSO events have existed for at least the past 130,000 yr, and that they continued even through glacial times. They also found that ENSO events of the 20th century were stronger than in past glacial or interglacial times. Cores from reef corals can frequently span centuries; Hendy et al. (2002) were able to go back in time more than 400 yr.

Most of the work on reef coral cores has emphasized temperature determinations, using the $\delta^{18}O$ paleothermometer. More than temperature can be determined from these cores, however, Fallon, White, and McCulloch (2002) used reef coral cores to determine the impact of mining on the waters around Misima Island, Papua New Guinea, and Heikoop, Tsujita, and Risk (1996) found the hydrothermal pulse associated with a volcanic eruption in the Banda islands, Indonesia, recorded in corals near the eruption site. As useful and as flexible as the reef coral record is, however, it suffers from severe geographical restrictions. To state the obvious, reef coral records may only be obtained where reef corals grow –– warm, shallow waters. The most dynamic oceanographic processes are frequently located deeper in the water column and further toward the poles.

The mid-90s saw increased interest in the records from deep-sea corals, sparked by two key papers. Druffel et al. (1995) determined an age of approximately 1,800 yr for an individual *Gerardia* (zoanthid) collected off Little Bahama Bank,

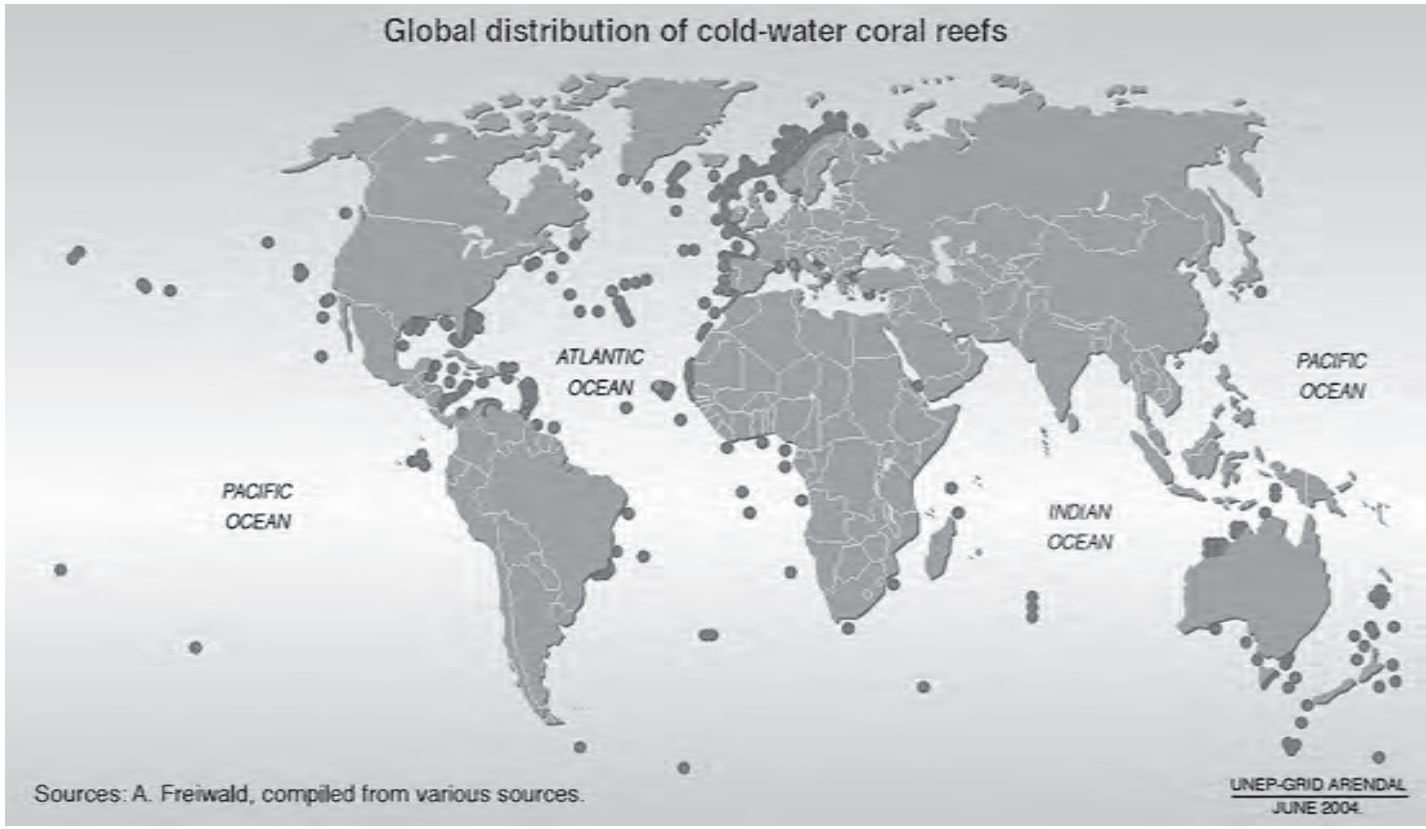

Figure 1 Global distribution of deep-sea coral reefs. Points on the map indicate observed reefs of varying size and stages of development but not the actual area covered. The high density of reefs shown in the North Atlantic reflects the intensity of research in this region. Further discoveries are expected worldwide, particularly in the deeper waters of subtropical and tropical regions. Figure from André Freiwald.

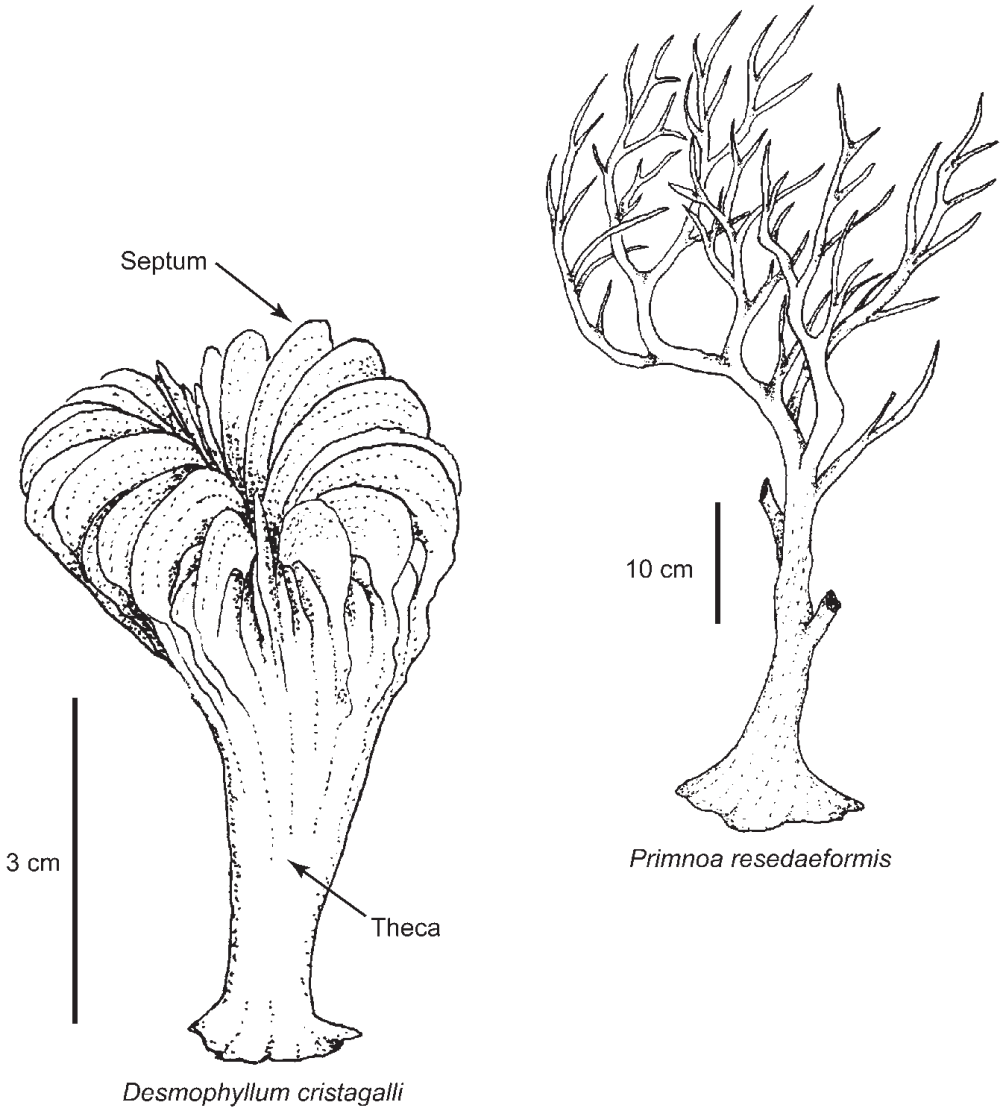

Figure 2 Two of the deep-sea scleractinian (*D. cristagalli*, a.k.a. *D. dianthus;* redrawn from Cairns, 1981) and horny corals (*P. resedaeformis*) discussed in this chapter.

suggesting that these organisms were perhaps the oldest living species in the ocean, rivaling Bristlecone Pines for the title of longest-lived organisms on the planet. They further suggested (p. 5031) "there is potential for *Gerardia* to serve as a millennial-scale integrator of upper ocean particle flux, and possibly reveal past changes in the productivity of the surface ocean." Smith, Risk, Schwarcz, and McConnaughey (1997) analyzed a suite of *Desmophyllum dianthus* from off Orphan Knoll, off the Newfoundland slope. The record of one pseudocolony captured a rapid cooling of intermediate waters at the onset of the Younger Dryas (~13 ka BP). Their analyses showed that this took place in as little as 5 yr, a startling find for the time.

The field has expanded dramatically in the past decade. At the Third International Symposium on Deep-Sea Corals, held in Miami in Nov–Dec 2005, there were climate-related papers from authors from almost 20 different countries.

1.2. Advantages of the Deep-Sea Coral Archive

To be accepted as dependable, any climate proxy extracted from organisms or sediments must be diagenetically stable, reproducible among specimens, and must faithfully record data of climatic significance. Advantages would be longevity, wide geographic and depth ranges, ease of analysis and abundance. Deep-sea corals fulfill all these criteria, with the possible exception of abundance. So-called deep-sea corals in fact range from depths of only a few meters (in places like Alaska and Chile), to >4 km, and in all oceans, but they are by no means abundant. In many cases, such as much of our own work, adventitious or opportunistic samples may be obtained from cultivating good relationships with fishermen, or from accidental trawl hauls. Samples specific to a given research project may be collected using deep submersibles, all of which are very expensive, and the use of which is mostly restricted to developed nations.

Although Scleractinians are relatively common and widespread in the deep-sea, obtaining long, coherent climate records from their skeletons can be challenging. They are usually small, less than 5 cm in height, and their growth banding is exceedingly narrow, *ca.* 10–100 μm (Lazier, Smith, & Risk, 1999; Sherwood, 2002). Recent technological advances, however, such as microsamplers and microprobes, have made small sample sizes much less of a problem, and, whereas a century of reef-coral record could be carried on a strong shoulder (it could weigh ~100 kg), the same length of record in a deep-sea coral could be tucked in a shirt pocket. In the future, it is likely that more research will focus on horny corals, which have tree-like morphologies, and lifespans of several centuries (Druffel, King, Belastock, & Buesseler, 1990; Druffel et al., 1995; Risk, Heikoop, Snow, & Beukens, 2002; Sherwood, Scott, & Risk, 2006).

In summary, deep-sea corals provide a widespread archive of oceanographic processes, with annual- to decadal-resolution records spanning several centuries in length. They are ideally suited to the study of rapid changes, such as that which characterized the Pleistocene–Holocene transition.

2. Methods and Interpretations

2.1. Growth and Sclerochronology in Deep-Sea Scleractinians

Deep-sea scleractinians exhibit a wide variety of growth forms, from simple, solitary cup corals to complex, branching colonies (Figure 2). A brief introduction to skeletal nomenclature is provided here, to facilitate the discussion of sclerochronology. The animal itself, the polyp, ranges from a few mm to several cm in diameter. The polyp sits atop a vertical calcified tube, the corallite, supported by a thin horizontal plate called the dissepiment. The corallite is lengthened by periodic

uplift of the polyp and formation of a new dissepiment. The wall of the corallite is called the theca. A series of thin vertical sheets, the septa, radiate from the theca into the center of the corallite.

At the microscopic scale, all the coral structures share a common mode of crystal nucleation and growth (see review in Cohen & McConnaughey, 2003). Crystals nucleate in so-called "centers of calcification" (COCs) producing randomly-oriented microgranules (Wainwright, 1964). In thin section, COCs appear opaque. Thickening of skeletal structures is achieved by the growth of crystal fibers outward from the COCs (Figure 3). Fan-shaped bundles of fibers (spherulites) take on an increasingly preferred orientation as they elongate (Barnes, 1970; Gladfelter, 1982). The fibrous region appears translucent in transmitted light, even though the crystals are more densely packed (Wainwright, 1964). Crystal fibers comprise the bulk of coral skeletons. Microbanding on the fibers occurs with a periodicity of *ca.* 1 μm (Sorauf & Jell, 1977). Cuif and Dauphin (2005) argued that fibers are not single crystals of aragonite, but rather composite structures built by the superposition of micron-thick layers, separated by an organic matrix.

Growth couplets consisting of alternating opaque-translucent band pairs (Figure 4) are found in many deep-sea scleractinians, ranging from 0.1 to 0.75 mm in width (Mortensen & Rapp, 1998; Lazier et al., 1999; Cheng, Adkins, Edwards, & Boyle, 2000; Adkins, Henderson, Wang, O'Shea, & Mokadem, 2004; Cohen et al., submitted). The delicate, sheet-like septae usually exhibit the clearest banding where they have not been secondarily thickened (Lazier et al., 1999). Growth bands are visible in transverse and longitudinal sections of the theca, but these may be susceptible to dissolution where the living tissue does not envelop the outer skeleton (Lazier et al., 1999). Cohen et al. (submitted) relate opaque-translucent

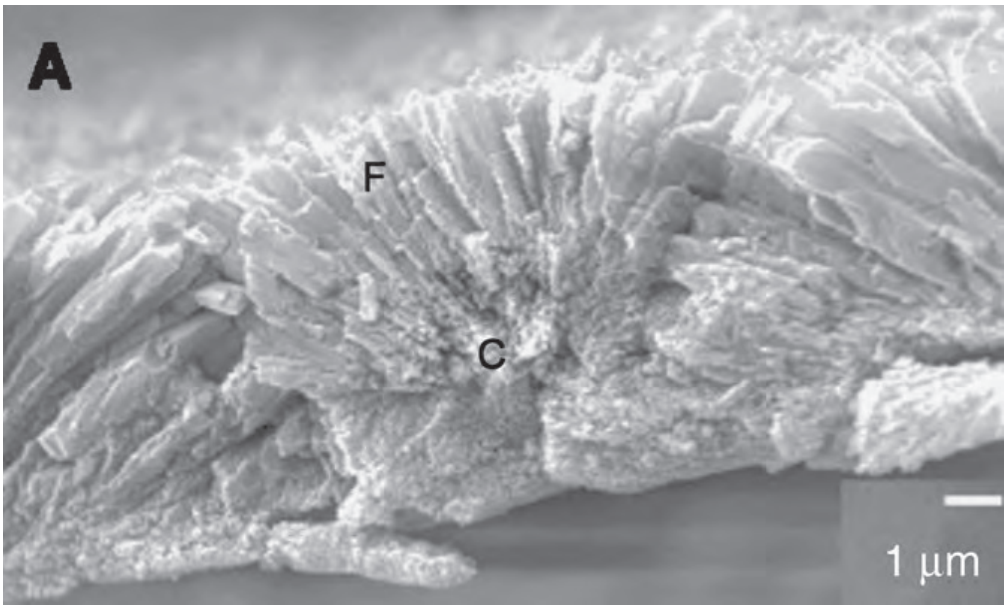

Figure 3 SEM image of centers of calcification (COC) and crystal fibers (F) in the (shallow-water) scleractinian coral *Porites lutea*. Note occlusion of crystal fibers at points of lateral interference. Image from Cohen and McConnaughey (2003).

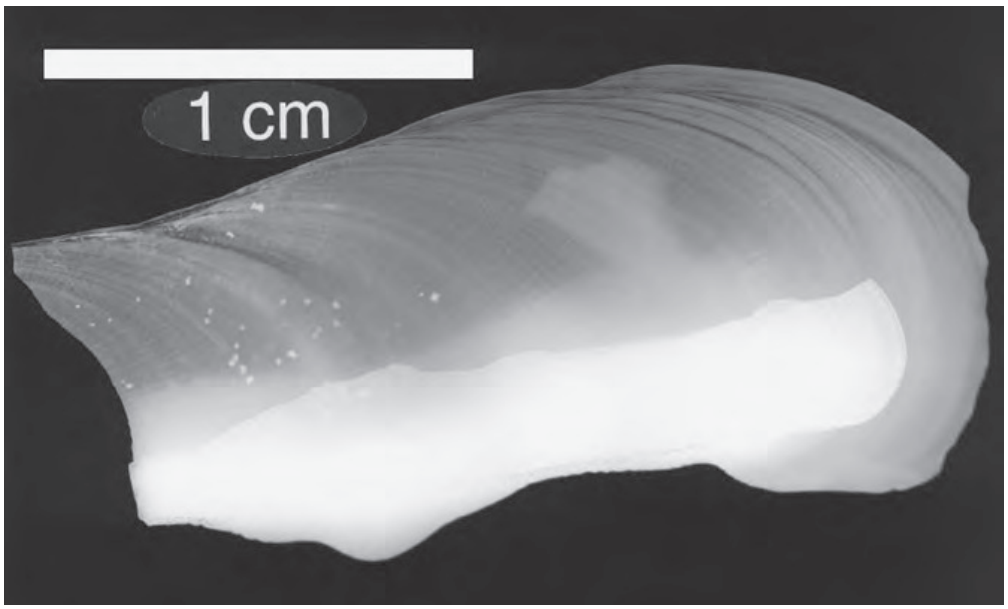

Figure 4 **Example of growth banding in a septum of the deep-sea scleractinian *Desmophyllum dianthus*. White patch at bottom of image is where the theca was attached. Figure from Cheng et al. (2000), with permission.**

growth banding observed in *Lophelia pertusa* to the repetition of crystal nucleation and growth events. They suggest that the process of crystal nucleation and growth occurs quickly in succession, and that it may reflect a seasonal growth spurt followed by a dormant period. Obviously, this has an important consequence for the continuity of geochemical proxy records.

The key utility of corals in paleoceanography is that long records of ambient conditions are locked into the growing skeleton in successive layers. When dealing with tropical reef scleractinians, massive colonies are selected for climate reconstructions because of the simplicity of their growth banding. Deep-sea scleractinians have more complicated cup and branching morphologies, making it difficult to visualize and sample the growth layers. The solitary cup corals are easier to deal with because they grow as one corallite over their 100+ yr lifespans (Smith et al., 1997; Adkins, Cheng, Boyle, Druffel, & Edwards, 1998; Cheng et al., 2000). Thus, the septa and theca exhibit the full complement of growth layers over the lifespan of the coral (Figure 4), provided that dissolution has not removed some of these layers (Lazier et al., 1999). Branching species are much more difficult to analyze because the individual corallites are relatively short lived. Although there are visible growth layers in the septa and theca of *Lophelia pertusa*, for example, they usually number <10 (Mortensen & Rapp, 1998; Cohen et al., submitted). Theoretically, extended chronologies could be developed by tracking successive growth layers into younger corallites, but this has not been demonstrated. Also, Pons-Branchu, Hillaire-Marcel, Deschamps, Ghaleb, and Sinclair (2005) raise the possibility that growth in *L. pertusa* occurs in relatively short bursts, separated by long hiatuses.

In most cases deep-sea corals cannot be observed growing in their natural habitat (but see Mortensen & Rapp, 1998), so growth rates must be determined

with radiometric dating techniques (e.g., U/Th, ^{226}Ra/Ba, ^{210}Pb or ^{14}C). Vertical growth rates range between 0.1 and 3 mm/yr for solitary corals (Cheng et al., 2000; Adkins et al., 2002; Adkins et al., 2004) and 2 and 5 mm/yr for branching corals (Mortensen & Rapp, 1998; Adkins et al., 2004). Corresponding periodicities of growth banding range from 0.3 to 3 bands/yr in *Desmophyllum dianthus* (Cheng et al., 2000) to ~0.1 bands/yr in *Enallopsammia rostrata* (Adkins et al., 2004). Banding periodicity probably varies within and among different species depending on depth and environmental conditions. For this reason, banding periodicity should be assessed on a case-by-case basis. Since they often live in near-constant physical conditions, the causes of growth banding in deep-sea scleractinians remains "quite literally, in the dark" (Lazier et al., 1999). Overall, it appears that growth banding in deep-sea scleractinians is not a reliable chronometer in most cases, and that skeletal chronologies must instead be established by radiometric dating methods.

2.2. Growth and Sclerochronology in Horny Corals

Several genera of deep-sea fans (Octocorallia: Order Gorgonacea) form durable, long-lived, tree-like skeletons (Figure 2). Compositionally, they differ from scleractinians in two key aspects. First, the carbonate phase is usually high magnesium calcite; some species deposit carbonate hydroxyapatite (Macintyre, Bayer, Logan, & Skinner, 2000). Relative to aragonite, the smaller lattice geometry of calcite favors co-precipitation of small cations such as Mg, and discriminates against larger cations, such as Sr and U. Second, the skeleton also contains a horny, fibrillar protein called gorgonin. The function of gorgonin is to lend flexibility to the otherwise stiff calcified skeleton (Grasshoff & Zibrowius, 1983; Lewis, Barnowski, & Telesnicki, 1992). Different regions of the skeleton may be composed of 'massive' (100%) calcite, 100% gorgonin, or a combination of both. For example, the Bamboo Corals (family Isididae) deposit gorgonin nodes, like the joints of a finger, between internodes of massive calcite. Red tree corals (family Primnoidae) deposit a two-part calcite-gorgonin "horny axis" towards the inner part of the axial skeleton, and a massive calcite cortex later on.

At the microscopic scale, massive calcite structures in octocorals appear almost identical to the aragonite in scleractinians (Lewis et al., 1992; Bond, Cohen, Smith, & Jenkins, 2005; Sherwood, 2002). Calcite fibers grow in spherulitic fashion, the fibers nucleating on gorgonin surfaces or COCs. Microbanding on the growing fibers occurs with a periodicity of *ca.* 1 μm. Where calcite is embedded with gorgonin, the calcite fibers take on stubbier morphologies, perhaps indicating a different process or rate of biomineralization.

Growth rings in octocorals may be observed in either the massive calcite or horny regions of the skeleton (Figure 5). In the massive calcite, the rings probably relate to the repetition of crystal growth and nucleation events (*sensu* Cohen et al., submitted). In the horny regions, the rings are produced by alternations in the ratio of gorgonin:calcite (Risk et al., 2002; Marschal, Garrabou, Harmelin, & Pichon, 2004; Sherwood, 2002), perhaps compounded by variations in the extent of protein tanning (Szmant-Froelich, 1974). Using bomb-^{14}C (Sherwood, Scott, Risk, & Guilderson, 2005a) and ^{210}Pb-dating (Andrews et al., 2002) annual ring periodicity

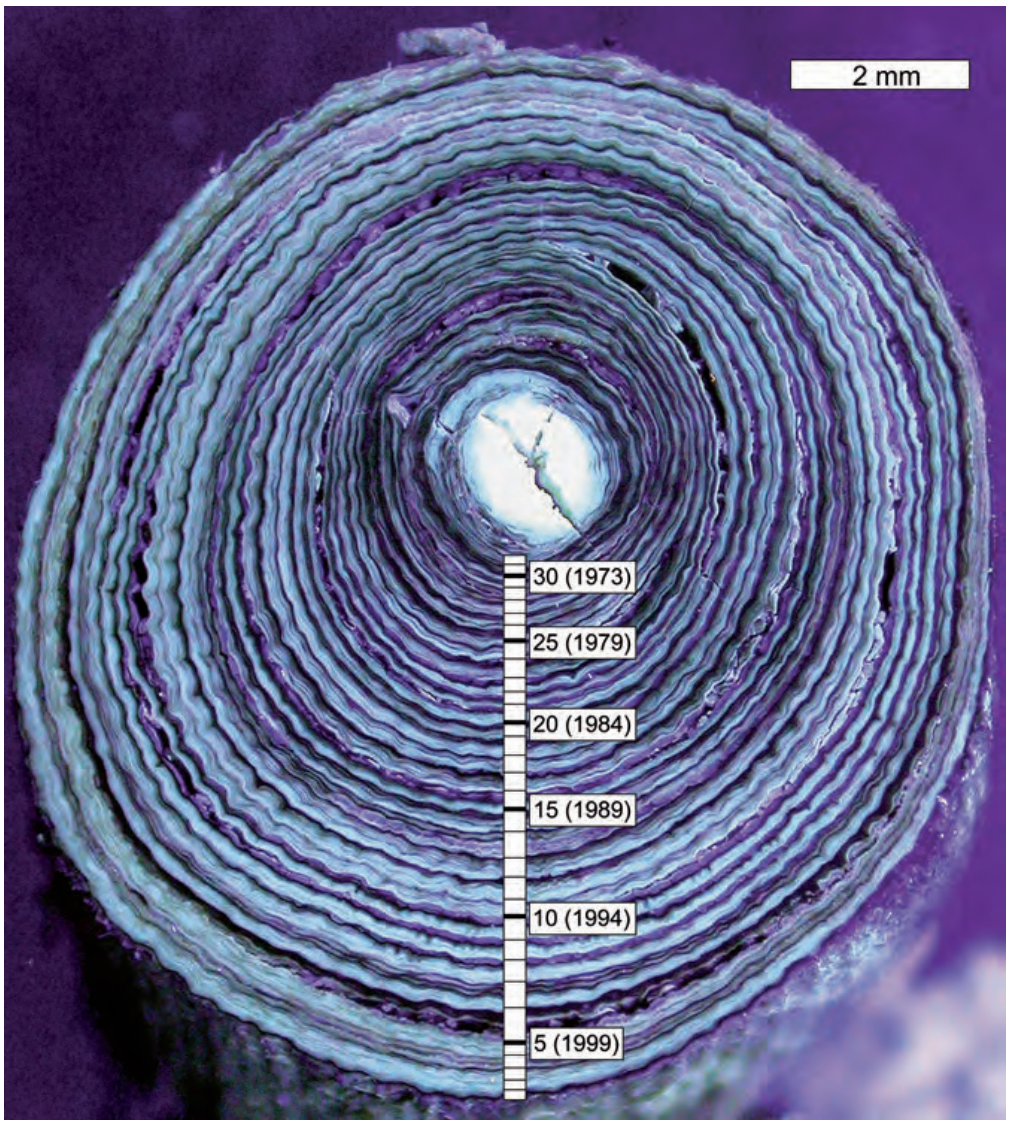

Figure 5 **Example of the annual growth rings in a young (30-yr-old) axial skeleton of the deep-sea gorgonian *Primnoa resedaeformis*. Markings show individual rings isolated for analysis, with corresponding calendar age (in brackets), as determined by amateur growth ring counters. Figure from Sherwood et al. (2005a), with permission.**

in the red tree coral *Primnoa resedaeformis* has been proven (Figure 6). Finer-scale growth rings, possibly lunar in origin, have also been described in *P. resedaeformis* (Risk et al., 2002; Sherwood, 2002) making this species perhaps the highest resolution deep water archive in the world. Thresher et al. (2004) verified annual ring formation in the calcite internodes of the bamboo coral *Keratoisis spp.* Other studies report more diffuse banding patterns, with ambiguous periodicities (Druffel et al., 1990; Roark et al., 2005; Andrews et al., 2005). As with scleractinians, it is highly likely that the appearance and timing of rings depends on local environmental factors, such as the downward flux of organic matter from spring plankton blooms

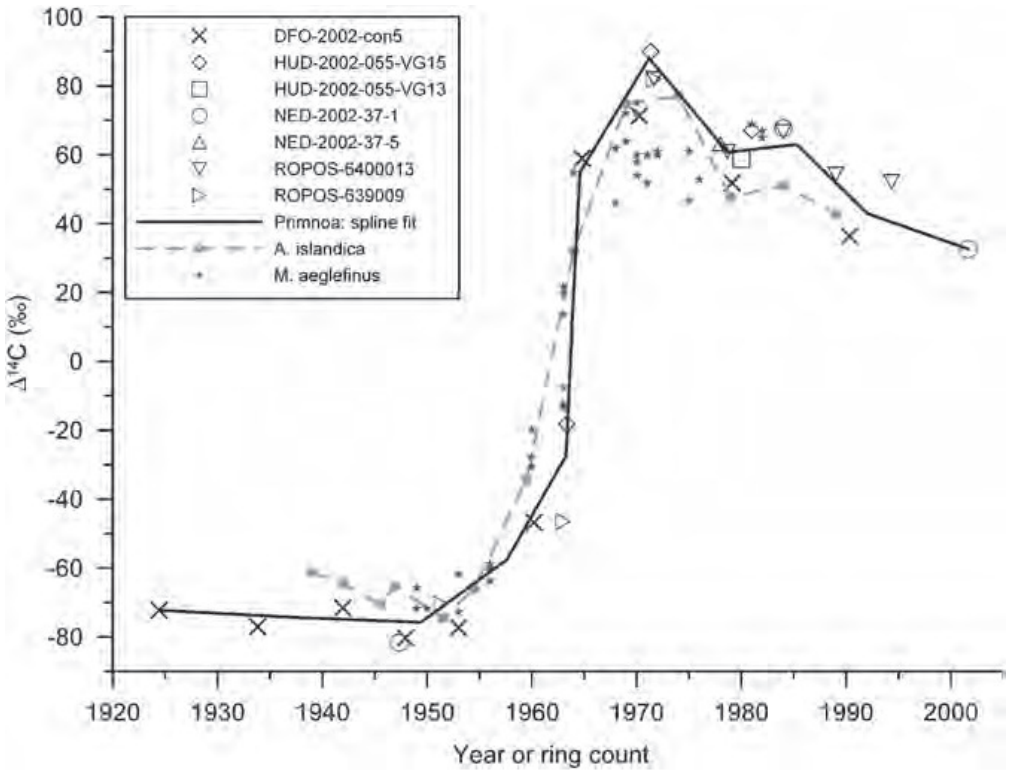

Figure 6 Timeseries $\Delta^{14}C$ of annual horny rings (after decalcification) of *Primnoa resedaeformis*. Data are from seven different colonies collected from 250 to 475 m in the NW Atlantic Ocean. Accurate reconstruction of the bomb ^{14}C signal proves annual ring periodicity. Reference curves for clam shell (*Arctica islandica*; Weidman & Jones, 1993) and haddock otoliths (*Melanogrammus aeglefinus*; Campana, 1997) also shown. Figure from Sherwood et al. (2005a), with permission.

(Sherwood, 2002). In regions of the ocean where seasonal variability is attenuated, growth rings may not be as prominently developed.

Lifespans of octocorals often exceed several hundreds of years (Druffel et al., 1990; Risk et al., 2002; Andrews et al., 2002; Thresher et al., 2004; Roark et al. 2005), the oldest reported lifespan being a 700 yr old specimen of *P. resedaeformis* (Sherwood et al., 2006). Compared with deep-sea scleractinian corals, obtaining centuries-long geochemical records from octocorals is simplified by the ability to sample across the growth rings of the axial skeletal.

Zoanthids and antipatharians (black corals) also show great promise as marine archives. These corals also form arborescent, concentrically banded skeletons composed of a horny protein much like the gorgonin found in octocorals (Goldberg, 1991; Druffel et al., 1995). The skeletons are not calcified, so the fossil record is sparse. However, these organisms have some of the longest lifespans of any corals. Druffel et al.'s (1995) 1,800-yr-old *Gerardia* is a case in point. Antipatharians may live for several hundreds of years (Williams, Risk, Sulak, Ross, & Stone, 2005), and their growth rings, demarcated by dark-colored protein "glue" (Goldberg, 1991), also appear to form annually (Williams et al., 2005).

2.3. Fossil Preservation

The degree of diagenetic stability of deep-sea corals seems excellent (Teichert, 1958). Repeated scanning electron microscope examination of deep-sea scleractinians from various depths (a few hundred meters to >2 km) and various oceans shows that they remain the original aragonite, with virtually no recrystallization, since the early Pleistocene (Titschak & Freiwald, 2005; Remia & Taviani, 2004). The massive calcite structures in gorgonians have more durable and compact skeletons; cretaceous-aged specimens are excellently preserved (Grasshoff & Zibrowius, 1983). The organic phase of horny corals has poorer preservation potential, but amino acid and stable isotopic analyses suggest that it is stable over at least the last few thousand years (Goodfriend, 1997; Sherwood et al., 2006).

Both the reef coral record and the deep-sea coral record, at least in the case of the scleractinian record, may be compromised by bioerosion. All corals, from all depths, are bored by a variety of organisms, of which the most prevalent are sponges and, in shallow water, algae. In deep-sea corals, the major bioeroders are sponges, fungi, bryozoa and polychaetes (Boerboom, Smith, & Risk, 1998; Bromley, 2005; Beuck & Freiwald, 2005; Wisshak, Freiwald, Lundälv, & Gektidis, 2005). The effects of bioerosion may range from complete removal of the record to selective dissolution of aragonite COCs (Titschak & Freiwald, 2005) and subtle alterations of the trace element composition of the skeleton (Pons-Branchu et al., 2005; Robinson et al., 2006). Virtually nothing is known of the process by which climate records are distorted by bioerosion.

2.4. Sources of Carbon to Deep-Sea Corals

Based on radiocarbon measurements, Griffin and Druffel (1989) originally established that the carbonate fraction of deep-sea scleractinians and octocorals is mostly derived from ambient dissolved inorganic carbon (DIC) at depth. Other authors have noted a 1:1 relationship in the $\Delta^{14}C$ of coral carbonate and seawater DIC (Goldstein, Lea, Chakraborty, Kashgarian, & Murrell, 2001; Adkins et al., 2002; Frank et al., 2004; Roark et al., 2005). Radiocarbon evidence limits the amount of respiratory CO_2 incorporated into the carbonate to $<10\%$ (Adkins et al., 2002); however, $\delta^{13}C$ data indicate that the amount of respired CO_2 may be somewhat higher in select species (e.g., Figure 7). QA :1

In contrast to the carbonate, the organic fraction of horny corals is synthesized from food sources sinking out of surface waters, a conclusion based on the presence of bomb-^{14}C in deep-dwelling specimens (Figure 6; Griffin & Druffel, 1989; Druffel et al., 1995; Roark et al., 2005; Sherwood et al., 2005a). The actual food sources are mostly unknown because field monitoring is prohibitively expensive, and specimens usually die when raised to the surface. Studies on relatively shallow-dwelling octocorals consistently point to detrital particulate organic matter (POM) and zooplankton (in a $\sim$50:50 ratio) as the main food sources (Ribes, Coma, & Gili, 1999, 2003; Orejas, Gili, & Arntz, 2003). The sinking, rather than suspended fraction of detrital POM is likely to be more important to deeper-dwelling taxa, as the nutritional value of the latter decreases with depth. Our $\Delta^{14}C$ and $\delta^{15}N$ data

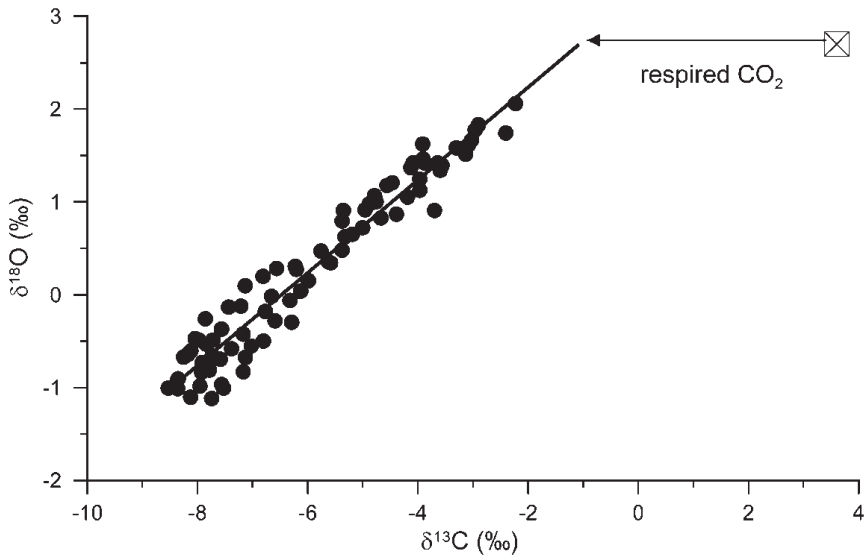

Figure 7 Stable isotopic data from a specimen of *Lophelia pertusa* collected from the NE Atlantic. Isotopic data plot along a straight line extending roughly to theoretical aragonite-seawater isotopic equilibrium (boxed cross). Horizontal offset from equilibrium is caused by skeletal incorporation of $\delta^{13}C$-depleted respired CO_2 (i.e., metabolic effects). Data from Risk, Hall-Spenser, and Williams (2005), with permission.

support a sinking POM and/or zooplankton (as both have approximately the same $\Delta^{14}C$ and $\delta^{15}N$) diet in deep-sea gorgonians and antipatharians, while ruling out deep suspended POM and dissolved organic matter (DOM) as important food sources (Heikoop, Hickmott, Risk, Shearer, & Atudorei, 2002; Sherwood et al., 2005a, 2005b; Williams et al., 2005).

2.5. Biocalcification Models

A debate on the mechanism of coral calcification has persisted for 40 yr (see review in Cohen & McConnaughey, 2003). A brief overview of this debate seems appropriate, as it frames our discussion of isotopic and trace elemental variability in coral carbonate. In the "organic matrix" model crystal growth is initiated, directed and terminated by organic secretions. Support for this idea is rooted in the detection of organic compounds within skeletal structures (Goreau, 1959; Johnston, 1980). More recently, the spatial distribution of sulfated polysaccharides within COCs and fibers has been worked out (Cuif & Dauphin, 2005). In the "physicochemical" model (Barnes, 1970; Constanz, 1986) crystal growth occurs freely within pockets of enzymatically-modified seawater beneath the ectodermal tissue. This idea is rooted in the similarity of spherulitic crystal morphology in corals to that in mineral specimens (Bryan & Hill, 1941).

One of the advantages of the physicochemical model is that, being grounded in the principles of inorganic (thermodynamic and kinetic) solution/crystal chemistry, it may be quantitatively evaluated against a growing body of isotopic and trace elemental data from coral skeletons (Sinclair & Risk, in press). These data indicate that isotopic and trace elemental compositions of corals almost always depart from

thermodynamic equilibrium (i.e., "vital effects"). However, physicochemical-based models can account for the isotopic and trace elemental disequilibria in corals through biological manipulation of calcification fluids without appealing to an organic matrix (McConnaughey, 1989b; Adkins, Boyle, Curry, & Lutringer, 2003; Sinclair, 2005; Sinclair & Risk, in press; Cohen et al., submitted).

In the classic model of calcification physiology (e.g., McConnaughey, 1989b; Cohen & McConnaughey, 2003) calcification occurs in a thin ($\sim$10 μm), extracellular calcifying fluid (ECF) between the coral tissue and the skeleton. The ECF is isolated from cell fluids by a membrane, which is permeable to small, uncharged molecules only. CO_2 passively diffuses across the cell membrane where it reacts with H_2O or OH^- to form HCO_3^-. The enzyme Ca-ATPase pumps Ca^{2+} into the ECF in exchange for two protons, to maintain charge neutrality. Proton removal increases the pH of the ECF, and converts HCO_3^- to CO_3^{2-}, which precipitates with Ca^{2+}. Small amounts of seawater HCO_3^- and $CO_3^=$, as well as trace elements, enter the ECF through leaky membranes or by passage of invaginated vacuoles across the cell membrane (Furla, Bénazet-Tambutté, Jaubert, & Allemand, 1998).

2.6. Stable Isotopic Disequilibria in Deep-Sea Corals

Oxygen and carbon isotope analysis of biogenic carbonates has been a cornerstone of paleoceanography for over 50 yr. The $\delta^{18}O$ of carbonate is used to infer past temperatures (Epstein, Buchsbaum, Lowenstam, & Urey, 1953) and the extent of continental glaciation (e.g., Shackleton, 1967), and $\delta^{13}C$ is used to identify water masses in the deep ocean (e.g., Sarnthein et al., 1994). Many biogenic carbonates that exhibit vital effects have consistent offsets from isotopic equilibrium. Deep-sea scleractinians are a special case; the extent of disequilibrium is highly variable within an individual coral (Emiliani et al., 1978; McConnaughey, 1989a; Smith, Schwarcz, Risk, McConnaughey, & Keller, 2000; Smith, Schwarcz, & Risk, 2002). When plotted in $\delta^{18}O$ vs. $\delta^{13}C$ space (Figure 7), isotopic data plot along straight lines extending roughly from equilibrium to a point up to 5‰ depleted for $\delta^{18}O$, and up to 15‰ depleted for $\delta^{13}C$. The slopes of these lines average $\sim$1/3. Octocoral calcites show similar patterns, though the extent of disequilibria is somewhat less (Druffel et al., 1990; Heikoop, Risk, Lazier, & Schwarcz, 1998).

According to McConnaughey's (1989b, 2003) kinetic model, strong isotopic depletions are mainly caused by hydration and hydroxylation of CO_2 within the ECF, although the pathways of $\delta^{18}O$ and $\delta^{13}C$ fractionation differ. For oxygen, both H_2O and OH^- are strongly depleted in $\delta^{18}O$: approximately -30‰ and -69‰, respectively. Since 1/3 of the oxygen atoms in HCO_3^- come from H_2O or OH^-, McConnaughey's (2003) calculations predict a DIC with a $\delta^{18}O$ composition well below that of aragonite in equilibrium with seawater. For carbon, the reaction of CO_2 with H_2O and OH^- strongly fractionates $\delta^{13}C$, approximately -7‰ and -27‰, respectively. Again, the resulting DIC takes on a $\delta^{13}C$ content much depleted compared with equilibrium aragonite. Hydroxylation of CO_2 predominates at pH $>$ 8, where most calcification occurs; thus, the stronger $\delta^{18}O$ and $\delta^{13}C$ depletions associated with hydroxylation dominate the isotopic composition of the coral skeleton (McConnughey, 2003).

McConnaughey (1989b) calculated that HCO_3^- could precipitate with Ca^{2+} much faster than it can attain equilibrium with H_2O in the ECF, so the $\delta^{18}O$ depletion is buried in the precipitating aragonite. Furthermore, equilibration of HCO_3^- occurs through a CO_2 intermediate, which diffuses back and forth across the cell membrane and equilibrates with cell H_2O at lower pH. Some of the carbon in the ECF is carried with the CO_2 molecule, allowing it to equilibrate within the cell also. Strong depletions in $\delta^{13}C$ incurred during hydration and hydroxylation are thereby partly "eroded" (Cohen & McConnaughey, 2003). The CO_2 molecule carries both C and O atoms across the cell membrane, allowing simultaneous equilibration of $\delta^{13}C$ and $\delta^{18}O$ in the cell. This accounts for the $\delta^{18}O$–$\delta^{13}C$ correlations in deep corals. In addition to "kinetic effects," a small amount of the CO_2 entering the ECF is derived from metabolism, and is ~2‰ depleted in $\delta^{13}C$ (McConnaughey, 1989a). Thus, the lines in $\delta^{18}O$–$\delta^{13}C$ space extend to a point roughly 2‰ depleted in $\delta^{13}C$ compared to equilibrium.

In recent years, a new aspect of isotopic disequilibria in deep-sea corals has emerged. High resolution microsampling reveals that COCs are more isotopically depleted than crystal fibers (Figure 8; Adkins et al., 2003; Rollion-Bard, Blamart, & Cuif, 2003). Moreover, isotopic data from COCs may even fall off the $\delta^{18}O$ vs. $\delta^{13}C$ lines, where $\delta^{18}O$ continues to decrease but $\delta^{13}C$ does not. Such anomalous data went unnoticed in earlier studies because the dental drills used in sampling could not be used to separate fibers from COCs (Lutringer, Blamart, Frank, & Labeyrie, 2005). To account for these observations, Adkins et al. (2003) developed a

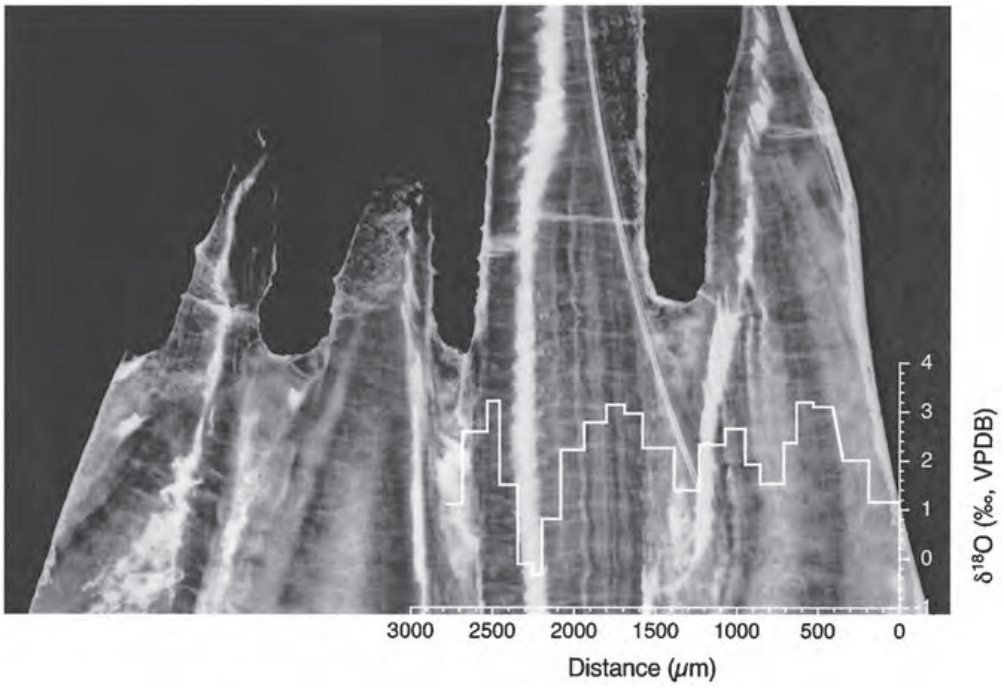

Figure 8 Transmitted light image of the thecal region of *Desmophyllum dianthus*, overlain with $\delta^{18}O$ results obtained with a high spatial resolution microsampler. Vertical line of COCs (lightest region) is associated with the lowest $\delta^{18}O$. Figure from Adkins et al. (2003), with permission.

"carbonate model" of isotopic disequilibrium. In their model, $\delta^{18}O$ and $\delta^{13}C$ disequilibria are driven by thermodynamic response to a biologically-induced pH gradient in the ECF. While McConnaughey's (1989b) kinetic model and Adkins et al.'s (2003) carbonate model are fundamentally different, both agree that isotopic depletions in COCs are an indication of a faster rate of calcification.

2.7. Overcoming Isotopic Disequilibria: The "Lines Technique"

Smith et al. (2000) proposed the "lines technique" as a way to overcome vital effects in deep-sea scleractinian corals. Their approach makes use of the fact that the lighter ends of $\delta^{18}O$–$\delta^{13}C$ regression lines for any one coral extend towards isotopic equilibrium (Figure 9). If $\delta^{13}C$ at equilibrium is known (from $\delta^{13}C$ of seawater or coeval benthic foraminifera), then, with a small correction for respiratory $\delta^{13}C$ (~2‰), the corresponding value of $\delta^{18}O$ at equilibrium, and hence temperature, can be calculated. Using 35 modern corals, Smith et al. (2000) showed that even if $\delta^{13}C$ is not known, the intercepts of $\delta^{18}O$–$\delta^{13}C$ regression lines were strongly correlated with temperature

$$(\delta^{18}O_c - \delta^{18}O_w) = -0.21\ T(^{\circ}C) + 4.51 \quad (1)$$

Equation (1) is nearly identical to Grossman and Ku's (1986) experimentally-

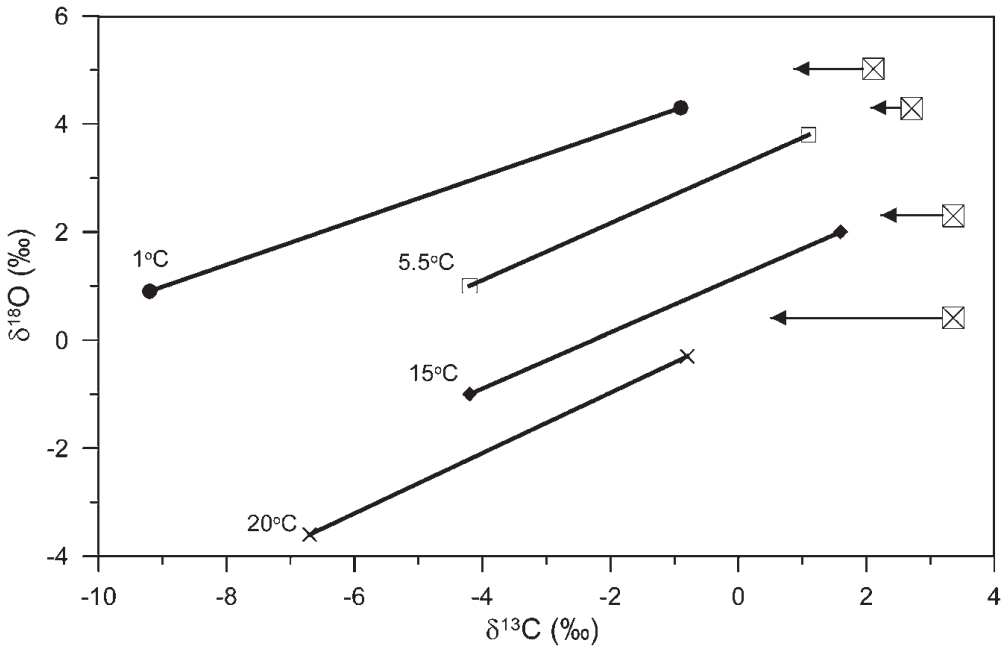

Figure 9 Isotopic data for four coral specimens collected from Antarctic shores, 410 m (solid circles); NW Atlantic slope, 1,025 m (open squares); NE Atlantic, 310 m (solid diamonds); Bahamas, 295 m (crosses). For clarity, only the least squares regression lines are shown. Crossed boxes represent theoretical isotopic equilibrium for each of the coral's datasets. Vertical offsets, reflecting temperature dependence of $\delta^{18}O$, are the basis for the 'lines technique'. Horizontal arrows point to intersection of regression lines with equilibrium $\delta^{18}O$; length of arrows reflects magnitude of theoretical metabolic effect. Figure modified from Smith et al. (2000), with permission.

derived $\delta^{18}O$ vs. temperature equation. This suggests that setting $\delta^{13}C = 0$ is a reasonable approximation for seawater $\delta^{13}C$ minus the respiratory $\delta^{13}C$ correction.

Weaknesses to the lines technique stem from variability in metabolic effects (Adkins et al., 2003), or the slopes of $\delta^{18}O$ vs. $\delta^{13}C$ (Smith et al., 2000). Despite these limitations, Smith et al. (2000) could calculate present day temperatures to a precision of ± 0.36 to $\pm 1^{\circ}C$ over a range of 1–28°C. The lines technique may not work as well with pre-Holocene corals, however, because seawater $\delta^{13}C$ was more variable, and coral metabolism may have been much different; this is apparent upon re-examination of their earlier results on *Desmophyllum* (Smith et al., 1997). In addition, Smith et al. (2000) used the classic dental drill sampling method, thus they did not take into account isotopic differences between fibers and COCs. Lutringer et al. (2005) analyzed fibers and COCs separately with an ion microprobe and essentially reproduced Smith et al.'s (2000) findings, albeit with slightly larger estimates of precision (± 0.7 to $\pm 1.5^{\circ}C$). Overall, the lines technique may be useful in tracking relatively large changes in water temperature, such as that which occurs in upper intermediate waters.

2.8. Trace Element Vital Effects

A growing body of evidence shows that trace elemental vital effects are a ubiquitous feature of shallow- and deep-water scleractinians alike (Sinclair et al., submitted). The mean compositions differ from inorganic carbonate, and the range of variability greatly exceeds that which can be accounted for by temperature-dependent partitioning alone. In scleractinians, different trace elements are strongly correlated with each other, much in the same way that $\delta^{18}O$ and $\delta^{13}C$ are correlated (Figure 10; Montagna, McCulloch, Taviani, Remia, & Rouse, 2005; Shirai et al., 2005; Sinclair et al., submitted). Moreover, elemental compositions are distinctly different in COCs than in surrounding fibers, with COCs being lower in Sr and U, and higher in Mg (Shirai et al., 2005; Gagnon & Adkins, 2005; Sinclair et al., submitted; Cohen et al., submitted). A recently developed trace element equilibrium/

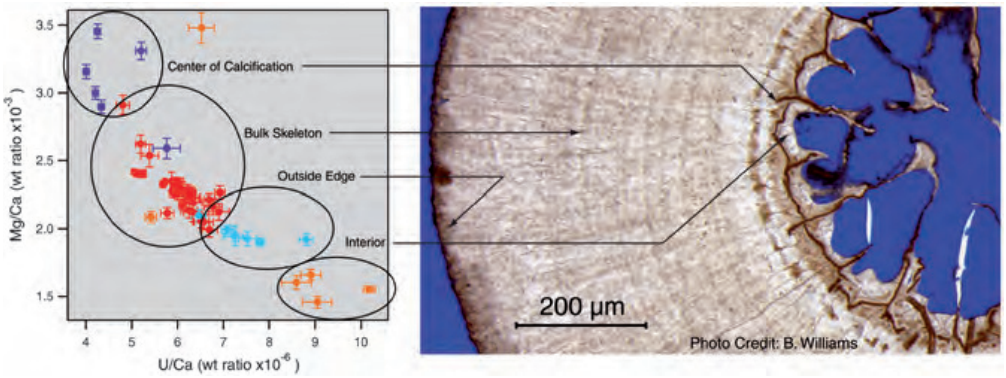

Figure 10 Negative correlation between Mg/Ca and U/Ca across the skeletal microstructures of *Lophelia pertusa*. Highest Mg and lowest U occurs in the optically dense COC. Conversely, the lowest Mg and highest U occurs in the optically light deposits that line the inside of the calyx. The bulk of the skeleton is a mixture between these two end-members. Figure from Sinclair et al. (submitted), with permission.

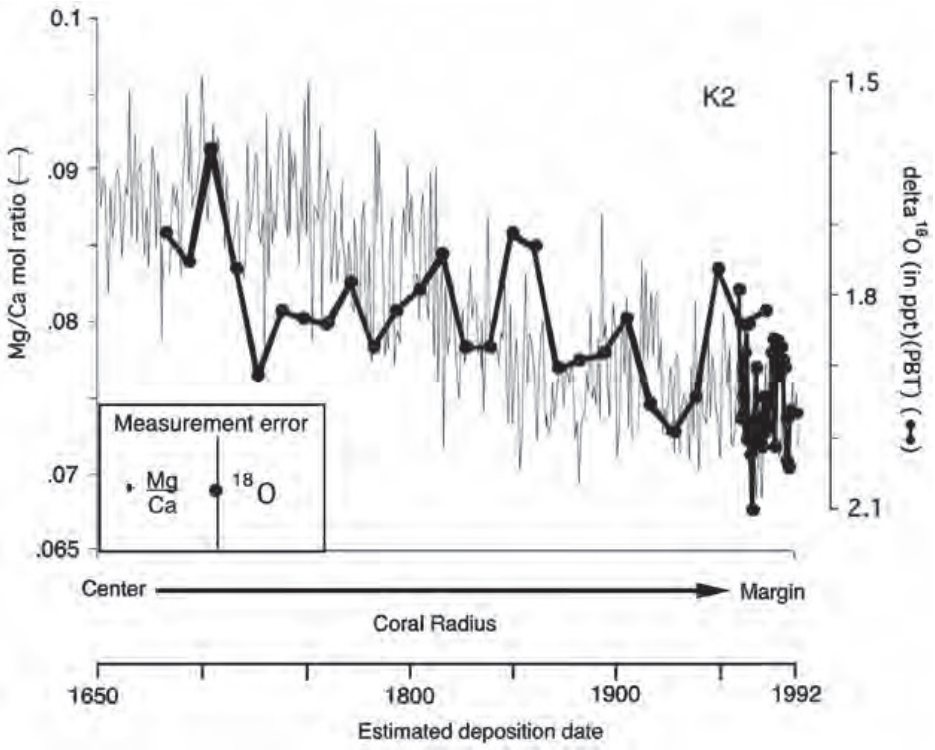

Figure 11 Records of Mg/Ca for a bamboo coral collected from ~1,000 m depth off Tasmania. Record of $\delta^{18}O$ is also shown. Both datasets indicate a gradual decline in water temperature over the last ~350 yrs. Figure from Thresher et al. (2004), with permission.

kinetic model of calcification can account for the apparent vital effects; specifically, Sr and U depletions are predicted at high calcification rates (Sinclair & Risk, in press). Cohen et al. (submitted) present evidence for a Sr/Ca paleothermometer in *Lophelia*; however, we are still a long way from producing reliable temperature reconstructions from scleractinian corals.

Following the extensive research on foraminiferal calcites, Mg/Ca in octocorals has been proposed as a potential paleothermometer (Weinbauer, Brandstätter, & Velimirov, 2000; Thresher et al., 2004; Bond et al., 2005; Sherwood et al., 2005c). Thresher et al. (2004) present 350 yr long records of Mg/Ca from Bamboo corals, which they interpret as evidence for recent cooling in the upper intermediate waters off Australia (Figure 11). More recent studies, however, suggest that Mg/Ca, as well as U/Ca and Sr/Ca, may be poorly reproducible along multiple transects of the same coral (Allard et al., 2005; Fallon, Roark, Guilderson, Dunbar, & Weber, 2005; Sinclair et al., 2005). Mg/Ca in particular may be strongly enriched in organic phases within the calcite, thus masking any temperature effect. On the other hand, Ba/Ca exhibits excellent reproducibility, and is therefore a good candidate as an environmental proxy (Allard et al., 2005; Fallon et al., 2005). Overall, further work is needed to assess the factors controlling elemental partitioning in octocoral calcite before reliable proxy data can be produced.

2.9. U-series Dating of Deep-Sea Corals

Deep-sea corals are excellent subjects for U-series dating. Scleractinians are easier to date because their aragonite skeletons contain higher levels of U (2–4 ppm) compared with the calcite skeletons of octocorals (3–4 ppb). With modern Multicollector ICP-MS, high precision U-series ages can be obtained on <1 g of sample. Here, we provide a brief overview of U-series dating as it applies to deep-sea corals. More detailed treatments are provided in Cheng et al. (2000) and Edwards, Gallup, and Cheng (2003). Both the ^{238}U–^{234}U–^{230}Th (U/Th) and the ^{235}U–^{231}Pa (U/Pa) decay schemes can be used. U/Th is the method of choice because it is somewhat more precise and covers a longer time range: 0–600 ka vs. 0–250 ka for U/Pa. However, U/Th dating can be used in concert with U/Pa (Goldstein et al., 2001), or even ^{226}Ra/Ba dating (Pons-Branchu et al., 2005), as a check on closed-system behavior and thus on dating accuracy.

In reef corals, it is normally the case that all of the measured ^{230}Th can be accounted for by radioactive in-growth. Deep-sea corals, on the other hand, live in a thorium-rich environment, since thorium increases with depth in the ocean. As a consequence, deep-sea corals may incorporate significant amounts of unsupported or non-radiogenic thorium, leading to older apparent ages. There are three sources of unsupported thorium (Cheng et al., 2000; Schröder-Ritzrau, Mangini, & Lomitschka, 2003): (1) a loosely attached detrital phase; (2) ferromanganese coatings, which adsorb thorium from seawater; and (3) an "initial", lattice-bound fraction incorporated during crystallization. The detritus and coatings can usually be removed by mechanical cleaning and by a series of chemical leaches, respectively (e.g., Shen & Boyle, 1988). Initial thorium cannot be separated from radiogenic thorium, so it must be accounted for in age calculations. The precision and accuracy of U/Th ages therefore depends on the precision and accuracy of the correction for unsupported thorium (Cheng et al., 2000).

The U/Th age equation, including the term for initial thorium is defined as (Edwards et al., 2003)

$$\{[^{230}U/^{238}U] - [^{232}U/^{238}U][^{230}Th/^{232}Th]_i\,(e^{-\lambda 230t})\} - 1 = -e^{-\lambda 230t} + \{\delta^{234}U_m/1000\}\{\lambda_{230}/(\lambda_{230} - \lambda_{234})\}\{1 - e^{-(\lambda 230 - \lambda 234)t}\} \quad (2)$$

where isotope ratios are activity ratios; λs are decay constants; t the ^{230}Th age; subscripts i and m represent initial and measured values, respectively; and $\delta^{234}U_m$ the measured deviation in per mil of the $[^{234}U/^{238}U]$ ratio from secular equilibrium $\delta^{234}U = ([^{234}U/^{238}U]-1) \times 1{,}000$. The measurement of ^{232}Th provides a check on the extent of unsupported thorium; thus, the only unknowns in equation (2) are the ^{230}Th age (t) and the initial $^{230}Th/^{232}Th$ activity ($[^{230}Th/^{232}Th]_i$).

There are two approaches to estimate $[^{230}Th/^{232}Th]_i$. In the first approach, a constant value is assumed, based on seawater measurements. This approach is suitable for relatively clean samples, with ^{232}Th contents of *ca.* <20 ppb. Cheng et al. (2000) showed that $[^{230}Th/^{232}Th]$ measured in modern deep-sea scleractinians from between 400 and 2,000 m in the Atlantic and Pacific Oceans was indistinguishable, within error, from seawater measurements. Their estimate of

$[^{230}Th/^{232}Th] = 14.8 +/- 14.8$ has been used as a "blanket" correction factor (Adkins et al., 1998; Cheng et al., 2000; Robinson et al., 2005). Alternatively, measurements of seawater $[^{230}Th/^{232}Th]$ specific to the area and depth of interest may be used to narrow the range of possible $[^{230}Th/^{232}Th]_i$ (Schröder-Ritzrau et al., 2003; Frank et al., 2004, 2005). Use of a constant $[^{230}Th/^{232}Th]_i$ correction assumes that seawater $[^{230}Th/^{232}Th$ was constant in the past, which may not necessarily have been the case. Accordingly, errors in $[^{230}Th/^{232}Th]_i$, of $\pm 50\%$ to 100% are propagated through the age calculations to account for this uncertainty.

The second approach, using the so-called Rosholt-II isochron method (Ludwig et al., 1994), assumes a two end-member mixing model between ^{232}Th-free carbonate and the ^{232}Th-rich contaminant (Lomitschka & Mangini, 1999; Schröder-Ritzrau et al., 2003, 2005). This method is suitable for heavily coated samples with ^{232}Th contents >20 ppb (Schröder-Ritzrau et al., 2005). Two to four fractions of the same sample are prepared and analyzed separately. The first fraction consists of just the coating; the other fractions are subjected to cleanings of increasing intensity, from simple mechanical cleaning to strong chemical leaching in ascorbic acid and Na_2EDTA solution (Lomitschka & Mangini, 1999). When plotted in $[^{230}Th/^{232}Th]$ vs. $[^{238}Th/^{232}Th]$ space, data for the different fractions define an isochron, the y-intercept of which represents the $[^{230}Th/^{232}Th]_i$ correction factor for input to equation (2). A slightly different variation of the isochron approach is outlined in Goldstein et al. (2001).

The relationship between measured and initial $\delta^{234}U$ is defined as (Edwards et al., 2003)

$$\delta^{234}U_m = (\delta^{234}U_i)e^{-\lambda 234 t} \quad (3)$$

If the ^{230}Th age can be solved independently, then Equation (3) can be used to calculate initial $\delta^{234}U$. Knowledge of $\delta^{234}U_i$ is a useful check on diagenetic alteration of the skeleton and hence open-system behavior, because marine $\delta^{234}U$ is fairly constant in time and space (Bard, Fairbanks, Hamelin, Zindler, & Chi Trach, 1991; Cheng et al., 2000; Henderson, 2002). If uranium is added to the skeleton by diagenetic processes (endolithic borings, secondary mineralization, microredox traps, pore water U; Swart & Hubbard, 1982; Pons-Branchu et al., 2005; Robinson et al., 2006), then the U/Th age equation may be invalidated. It is common practice to discard data when $\delta^{234}U_i$ falls outside a defined range of seawater $\delta^{234}U$ (e.g., 146 ± 7‰; Robinson et al., 2005).

Compilation of all published U/Th dates in deep-sea scleractinians provides an indication of the accuracy and precision of the technique (Figure 12). In general, $^{230}Th/^{232}Th$-corrected ages are younger than uncorrected ages by $<3\%$. Thus, depending on the dating resolution required, a correction may not be necessary, provided that the ^{232}Th concentration is low. For uncorrected ages, the 2σ dating precision is better than 1%. For corrected data, the 2σ precision is larger, $\sim 5\%$, owing to uncertainty in the value of initial $[^{230}Th/^{232}Th]$. There are no apparent differences in the precision of the isochron vs. non-isochron dating techniques.

In summary, U/Th dating of deep-sea corals is challenging because of the presence of unsupported Th, which leads to older apparent ages, and possible diagenetic incorporation of U, leading to younger apparent ages. With careful

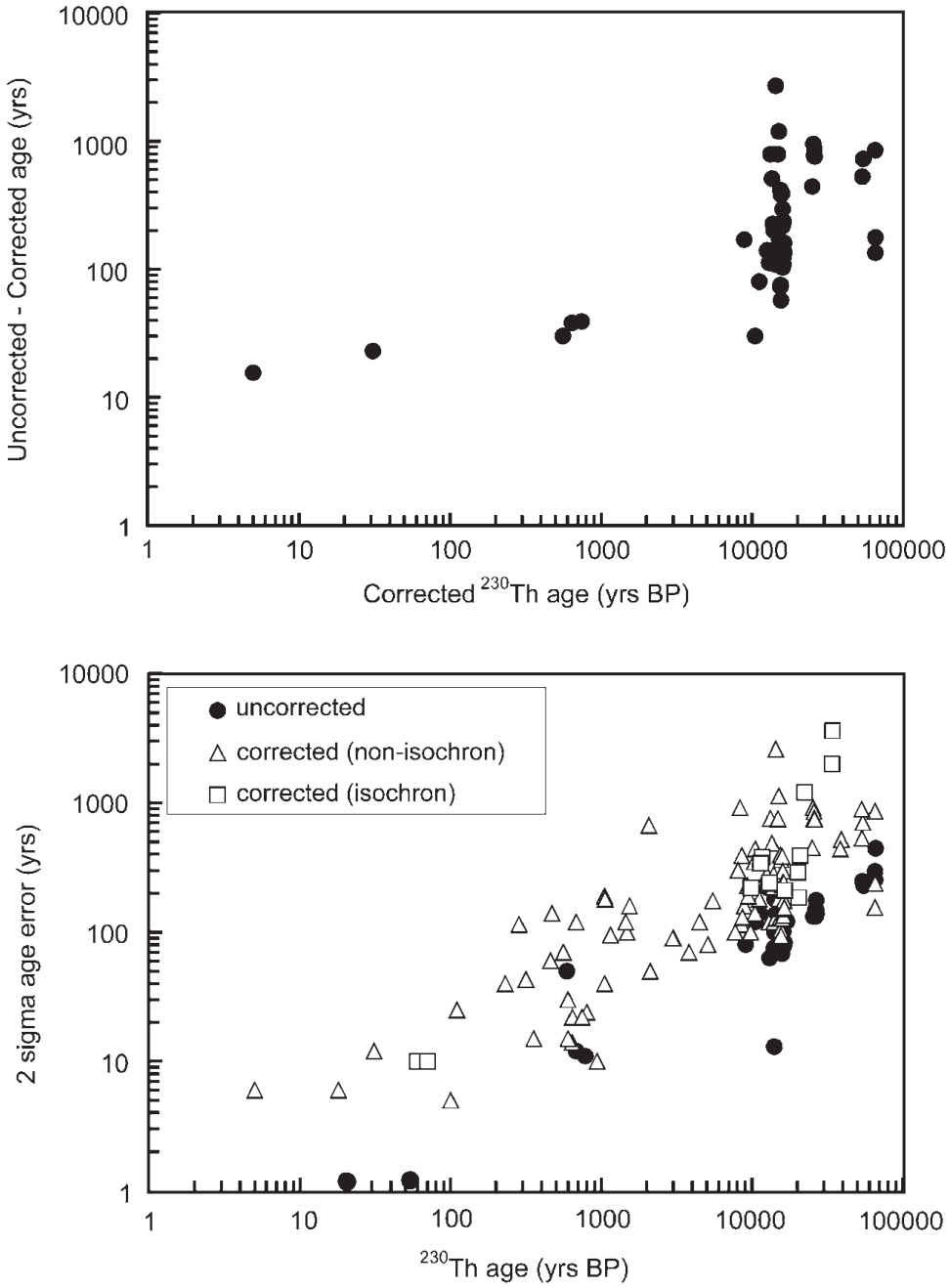

Figure 12 Compilation of all published U/Th dates from deep sea scleractinian corals. Upper panel: Difference between uncorrected and corrected ages averages <3%. Lower panel: 2σ age errors associated with uncorrected data, and corrected data using either the isochron or non-isochron approaches. See text for explanation.

sample pre-treatment, correction for unsupported Th, and screening for diagenetically-altered samples, high precision U/Th dates may be obtained.

2.10. Radiocarbon Dating and Paleo-$\Delta^{14}C$

Seawater $\Delta^{14}C$ has long been recognized as an important tool for tracking water mass circulation (Key, 2001). In the deep North Atlantic, for example, $\Delta^{14}C$ differentiates North Atlantic Deep Water (−65‰) from Antarctic Bottom Water (−165‰; Broecker, Gerard, Ewing, & Heezen, 1960; Stuiver, Quay, & Ostlund, 1983). The relative dominance of these water masses at any one location provides an indication of oceanic circulation patterns. Coral skeletons provide one of the few archives of past seawater $\Delta^{14}C$ variations, since their carbonate skeletons are derived from ambient DIC at depth (Griffin & Druffel, 1989; Adkins et al., 2002).

Coral skeletons contain enough carbonate material to perform both U/Th and ^{14}C dating on the same sample (Adkins et al., 1998; Mangini, Lomitschka, Eichstadter, Frank, & Vogler, 1998). Since the U/Th-dating can be used to calculate an absolute age, paired U/Th-^{14}C dating provides a direct measure of the ^{14}C age of the seawater in which the coral grew (Bard, Arnold, Fairbanks, & Hamelin, 1993; Edwards et al., 1993; Adkins et al., 2002). Adkins et al. (1998) and Mangini et al. (1998) first demonstrated this method on deep-sea corals, analogous to the method of differencing radiocarbon ages from pairs of benthic-planktic foraminifera sampled from the same core interval (B/P-dating; Broecker et al., 1990), but much improved by the fact that bioturbation and foraminiferal species effects are not at issue, and U/Th dating is model independent.

Paleo-$\Delta^{14}C$ may be calculated by (Adkins & Boyle, 1997)

$$\Delta^{14}C_{\text{paleo}} = \left\{ \frac{e(-^{14}\text{C age}/8033)}{e(-\text{cal age}/8266)} \right\} - 1 \times 1000 \quad (4)$$

where ^{14}C age is the ^{14}C age measured on the coral, cal age is the U/Th age measured on coral, 8,033 is the Libby mean life and 8,266 is the true ^{14}C mean life in years. Knowledge of paleo-$\Delta^{14}C$ is powerful for tracking past variations in deep and intermediate water mass distributions (Frank et al., 2004, 2005; Robinson et al., 2005). In theory, by projecting paleo-$\Delta^{14}C$ values back in time to their intersection with the atmospheric record, the residence time or ventilation age of deep water masses may be calculated (Adkins et al., 1998; Mangini et al., 1998; Goldstein et al., 2001; Schröder-Ritzrau et al., 2003); however, this approach may be complicated by the mixing of multiple water masses with different convection histories.

2.11. Surface Signals from the Organic Skeletons of Horny Corals

Some of the more promising paleoceanographic information may found in the skeletons of horny corals. Druffel et al. (1995) originally hypothesized that certain aspects of export of POM may be monitored by studying the isotopic and amino acid chemistry of horny layers, in much the same way that down-core trends in sedimentary organic matter (SOM) is utilized in paleoceanography. In some species the annual rings may be decalcified and gently peeled apart and analyzed separately, without the need for expensive *in situ* microprobe analyses. Moreover, the amino acid composition of the horny material is stable over at least the last few thousand

years, an indication that it is resistant to organic diagenesis (Goodfriend, 1997; Sherwood et al., 2006). Since the horny material is derived from sinking POM and/or zooplankton, annually banded horny corals provide a long-term, high resolution archive of biogeochemical processes occurring in surface waters (Sherwood et al., 2005b).

Accurate reconstruction of 20th century bomb radiocarbon from *Primnoa resedaeformis* (Figure 6) is a good example of the type of data that may be retrieved from horny corals (Sherwood et al., 2005a). As a variation on B/P dating, paired ^{14}C dating of both the carbonate and horny phases may prove to be useful in tracking ventilation rates of ambient water masses. The $\delta^{15}N$ and $\delta^{13}C$ of the horny phase may be another source of paleoceanographic data (Heikoop et al., 2002; Sherwood et al., 2005b; Ward-Paige, Risk, & Sherwood, 2005; Williams et al., 2005). The $\delta^{15}N$ and $\delta^{13}C$ in gorgonians and antipatharians is correlated with $\delta^{15}N$ and $\delta^{13}C$ in phytoplankton. Moreover, the intra- and inter-colony reproducibility of both isotopes appears to be excellent.

The $\delta^{15}N$ composition of horny corals is controlled by a variety of bottom-up processes, beginning with the isotopic composition of source nutrients, uptake by phytoplankton, and the length and complexity of the food web. The relative influence of denitrification vs. nitrification among different oceanographic regimes has a strong impact, for example, on the $\delta^{15}N$ of NO_3 (Cline & Kaplan, 1975; Altabet et al., 1999; Knapp, Sigman, & Lipschultz, 2005). Phytoplankton preferentially assimilate $^{14}NO_3$, leading to isotopically depleted biomass. In many regions of the ocean NO_3 is completely consumed, and the $\delta^{15}N$ of phytoplankton and sinking POM converges on the $\delta^{15}N$ of subsurface NO_3 (Altabet & McCarthy, 1985; Altabet, 1988; Altabet et al., 1999; Thunell, Sigman, Muller-Karger, Astor, & Varela, 2004). This is the basis for the interpretation of down-core sedimentary QA :4
$\delta^{15}N$ as a proxy for the $\delta^{15}NO_3$ history of the oceans (Altabet, Francois, Murray, & Prell, 1995; Ganeshram, Pederson, Calvert, & Murray, 1995; Haug et al., 1998). The simple relation between subsurface NO_3 and sinking POM may be confounded by a variety of factors, including incomplete nutrient utilization (Altabet & Francois, 1994), alteration of sinking POM during transit through the water column (Saino & Hattori, 1987; Altabet, Deuser, & Honjo, 1991), and the complexity of the plankton food web (Altabet, 1988; Wu, Calvert, & Wong, 1999a). This latter factor presents the largest source of uncertainty in the interpretation of $\delta^{15}N$ data from horny corals, since trophic fractionation is large (~3.4‰ per trophic level; DeNiro & Epstein, 1981) relative to oceanic $\delta^{15}NO_3$ variability, and the corals may feed opportunistically on a wide range of plankton size classes (Ribes et al., 1999, 2003; Orejas et al., 2003). Future compound-specific isotope analyses will likely allow for the separation of trophic level and source nutrient isotope effects through separate analysis of different amino acids (McClelland & Montoya, 2002).

Specific processes that could be tracked with the $\delta^{15}N$ composition of horny corals include water mass movements, eutrophication, and trophic dynamics. Recent exploratory studies highlight some of this potential, particularly in assessing anthropogenic perturbations over the last few centuries. Sherwood (2006) presented a near 2,000-yr-long record of $\delta^{15}N$ from colonies of *P. resedaeformis* collected from the slope water region off eastern Canada (Figure 13). Anomalous

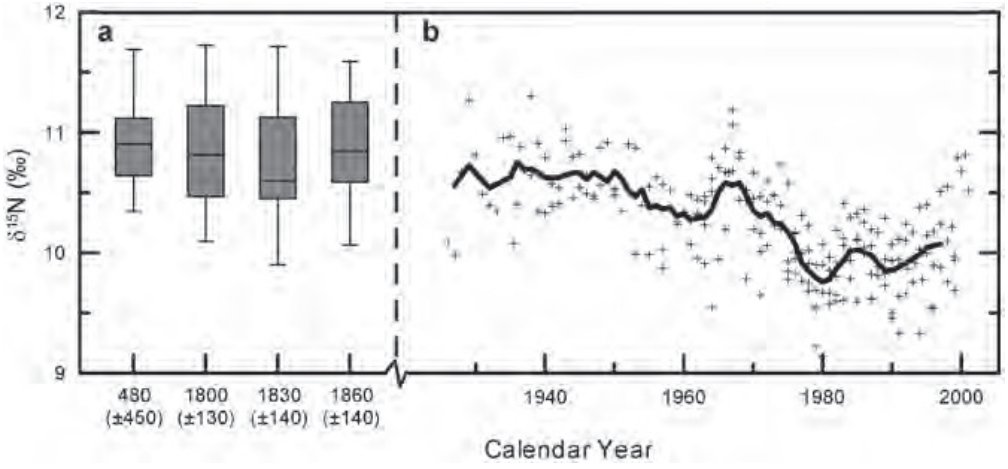

Figure 13 δ^{15}N measured in the annual horny rings of *Primnoa resedaeformis* (NW Atlantic; 250–475 m). (a) Data for subfossil colonies plotted as box-and-whisker plot because of uncertainties in radiocarbon age calibrations. Each box represents at least 20 annual rings. Numbers below boxes indicate mean calibrated ^{14}C age ($\pm 2\sigma$ range). (b) Data for six recent colonies plotted against calendar year, as dated by the bomb-^{14}C method and visual counting of annual rings. Bold line indicates 5 yr running mean. The 20th century decline in δ^{15}N is attributed to isotopic depletion of ambient NO_3, and/or trophic level effects. From Sherwood (2006), with permission.

decline in δ^{15}N over the 20th century was interpreted to reflect weakening of isotopically-heavier Labrador Current, or a change in the relative trophic level of the corals. Ward-Paige et al. (2005), using shallow gorgonians, and Williams et al. (2005), using deep antipatharians, presented records of long-term increases in δ^{15}N off SE USA, which they interpreted as evidence of increasing anthropogenic nutrient inputs.

The δ^{13}C of horny corals is controlled by a different assortment of bottom-up processes. Variability in the δ^{13}C of oceanic DIC is only 1–2‰ (Kroopnick, 1985), and trophic fractionation averages only ~1‰ per trophic level (DeNiro & Epstein, 1978). The δ^{13}C of SOM is often used to distinguish between marine and terrestrial inputs (Fry & Sherr, 1984); however, this generally does not apply to deep corals because they usually inhabit regions far from terrestrial influences. Most of the variability in δ^{13}C of phytoplankton and subsequent trophic levels arises from isotopic fractionation during phytoplankton growth. Earlier studies emphasized dissolved CO_2 in determining phytoplankton δ^{13}C, and the use of sedimentary δ^{13}C as a proxy for paleo-CO_2 (Jasper, Hayes, Mix, & Prahl, 1994; Rau, 1994). More recent studies point to growth rate, cell geometry, nutrient and light limitation and active carbon uptake (as opposed to diffusive uptake of CO_2) as equally, if not more important determinants of δ^{13}C (see review in Laws, Popp, Cassar, & Tanimoto, 2002). Long-term declines in δ^{13}C measured in octocorals and antipatharians appear to reflect the oceanic Suess effect, that is, the gradual depletion of oceanic δ^{13}C due to burning of isotopically-light fossil fuels (Williams et al., 2005; Sherwood, 2006). Over shorter time periods, the observed variations are yet to be explained. As with δ^{15}N, future compound-specific analysis may lead to a better understanding of δ^{13}C records obtained from horny corals.

3. Landmark Studies

Having explored the growth, geochemistry and radiometric dating of deep-sea corals, we now turn our attention to a few studies that have produced operationally useful paleoceanographic data. We focus on papers dealing with the rate of intermediate water mass variability across the Pleistocene–Holocene transition. The central theme of these papers is that climatic transitions occur over very short (decadal) timescales. Under most circumstances decadal-scale events are difficult to reconstruct from marine sediment records because of bioturbation.

Smith et al.'s (1997) landmark paper focused on *Desmophyllum* corals collected from the top of Orphan Knoll (1,800 m), an isolated seamount off the Newfoundland slope. The location and depth of Orphan Knoll allowed for the reconstruction of intermediate water mass variability in the Labrador Sea, an important component of the North Atlantic circulation. Stable isotopic data from these corals exhibited a major difference in the distribution of $\delta^{18}O$ vs. $\delta^{13}C$ lines between warm and cold periods spanning the last 15 ka (Figure 14). Foreshadowing the 'lines technique' published a few years later (Smith et al., 2000), they assumed that the lighter ends of their $\delta^{18}O$ vs. $\delta^{13}C$ lines approached isotopic equilibrium with seawater, an assumption supported by similarity of $\delta^{18}O$ values measured in contemporaneous foraminifera. One of their corals captured a rapid shift from warmer conditions at the base of the coral (13.400 ka BP), to cooler conditions at the top of the coral (13.322 ka), approximately co-incident with the accepted timing of the onset of the Younger Dryas event (12.9 ka BP). In this specimen, the shift from full

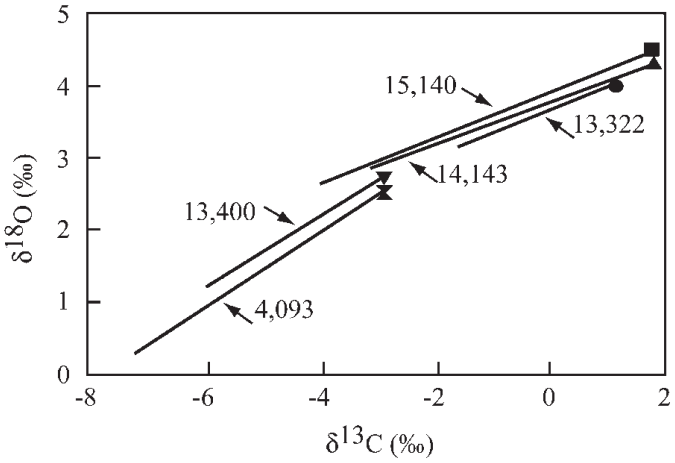

Figure 14 Isotopic data from *Desmophyllum dianthus* collected from Orphan Knoll (Labrador Sea). For clarity, only the least squares regression lines are shown. Symbols indicating isotopic maxima for each of the coral's datasets are assumed to approach isotopic equilibrium. Numbers indicate U/Th ages in years BP. The two oldest corals (15,140 and 14,143 yr) grew when the Labrador Sea retained much of its glacial character. Corresponding $\delta^{18}O$ maxima average 4.5‰. At the base of the next youngest coral (13,400 yr), $\delta^{18}O$ maxima (2.5‰) are much like that of a mid-Holocene coral (4,093 yr). Further up the same colony (13,322 yr), data return to that of the oldest-aged corals, indicating a rapid return to glacial-like conditions with the onset of the Younger Dryas. Figure from Smith et al. (1997), with permission.

warm to full cold conditions occurred between subsamples spaced 3 mm apart, an equivalent of 5 yr in time. This study was the first to demonstrate the utility of deep-sea corals in providing useful paleoceanographic data.

Shortly thereafter, a series of papers on paired U/Th-^{14}C dating of deep-sea corals came out, emphasizing rapid changes in intermediate water ventilation rates across the Pleistocene–Holocene transition (Adkins et al., 1998; Schröder-Ritzrau et al., 2003). The approach outlined in these studies culminated in the recent work of Robinson et al. (2005), with data from some 30 corals recovered from the New England Seamounts (33–39°N). Their reconstructions of paleo-Δ^{14}C over the interval 11–25 ka (Figure 15) document switches in the relative proportions of southern vs. northern source waters (a "bipolar seesaw"). Switches at intermediate depths occurred more frequently than they did in the abyss, and they coincided with climatic events documented in Greenland and Antarctic ice cores. The 15.4 ka event, in particular, saw a shift from full glacial to full modern-like conditions that took place in less than 100 yr.

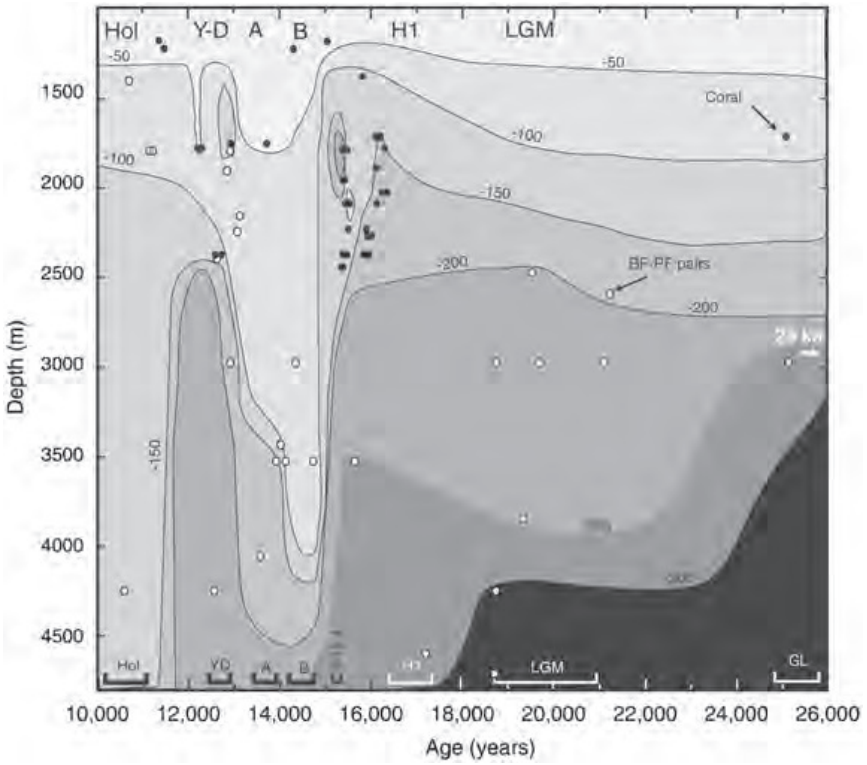

Figure 15 Mid-North Atlantic paleo-Δ^{14}C reconstructed from deep-sea corals (black circles) and foraminifera B/F pairs (white circles). During the last glacial period and Younger Dryas, the deep ocean was dominated by older, Δ^{14}C-depleted southern source waters, indicating cessation of deep water formation in the N. Atlantic. Younger, northern source waters characterize the warmer Bølling–Allerød and Holocene periods. Coral data indicate higher frequency variability in upper intermediate waters. Figure from Robinson et al. (2005), with permission.

Uncited references

Ludwig & Titterington (1994); Sigman, Altabet, McCorkle, Francois, & Fischer (2000).

REFERENCES

Adkins, J. F., & Boyle, E. A. (1997). Changing atmospheric $\Delta^{14}C$ and the record of deep water paleoventilation ages. *Paleoceanography, 12*, 337–344.

Adkins, J. F., Boyle, E. A., Curry, W. B., & Lutringer, A. (2003). Stable isotopes in deep-sea corals and a new mechanism for "vital effects". *Geochimica et Cosmochimica Acta*, *67*, 1129–1143.

Adkins, J. F., Cheng, H., Boyle, E. A., Druffel, E. R. M., & Edwards, R. L. (1998). Deep-sea coral evidence for rapid change in ventilation of the deep North Atlantic 15,400 years ago. *Science*, *280*, 725–728.

Adkins, J. F., Griffin, S., Kashgarian, M., Cheng, H., Druffel, E. R. M., Boyle, E. A., Edwards, R. L., & Shen, C.-C. (2002). Radiocarbon dating of deep-sea corals. *Radiocarbon*, *44*, 567–580.

Adkins, J. F., Henderson, G. M., Wang, S.-L., O'Shea, S., & Mokadem, F. (2004). Growth rates of the deep-sea scleractinian *Desmophyllum cristagalli* and *Enallopsammia rostrata*. *Earth and Planetary Science Letters*, *227*, 481–490.

Allard, G., Sinclair, D. J., Williams, B., Hillaire-Marcel, C., Ross, S., & Risk, M. (2005). Dendochronology in bamboo? Geochemical profiles and reproducibility in a specimen of the deep water bamboo coral *Keratoisis* spp. *Proceedings of 3rd International Symposium Deep-Sea Corals* (p. 204). Miami, USA.

Altabet, M. A. (1988). Variations in nitrogen isotopic composition between sinking and suspended particles: Implications for nitrogen cycling and particle transformation in the open ocean. *Deep Sea Research*, *35*, 535–554.

Altabet, M. A., Deuser W.G., Honjo,S., & Honjo, S. (1991). Seasonal and depth-related changes in the source of sinking particles in the North Atlantic. *Nature*, *354*, 136–139.

Altabet, M. A., & Francois, R. (1994). Sedimentary nitrogen isotopic ratio as a recorder for surface ocean nitrate utilization. *Global Biogeochemical Cycles*, *8*, 103–116.

Altabet, M. A., Francois, R., Murray, D. W., & Prell, W. L. (1995). Climate-related variations in denitrification in the Arabian Sea from sediment $^{15}N/^{14}N$ ratios. *Nature*, *373*, 506–508.

Altabet, M. A., & McCarthy, J. J. (1985). Temporal and spatial variations in the natural abundance of ^{15}N in PON from a warm-core ring. *Deep Sea Research*, *32*, 755–772.

Altabet, M. A., Pilskaln, C., Thunell, R., Pride, C., Sigman, D., Chavez, F., & Francois, R. (1999). The nitrogen isotope biogeochemistry of sinking particles from the margin of the eastern North Pacific. *Deep Sea Research*, *46*, 655–679.

Andrews, A. H., Cailliet, G. M., Kerr, L. A., Coale, K. H., Lundstrom, C., & DeVogelaere, A. P. (2005). Investigations of the age and growth for three deep-sea corals from the Davidson Seamount off central California. In: A. Freiwald & J. M. Roberts (Eds), *Cold-Water Corals and Ecosystems* (pp. 1021–1038). Berlin: Springer.

Andrews, A. H., Cordes, E. E., Mahoney, M. M., Munk, K., Coale, K. H., Cailliet, G. M., & Heifitz, J. (2002). Age, growth and radiometric age validation of a deep-sea, habitat-forming gorgonian (*Primnoa resedaeformis*) from the Gulf of Alaska. *Hydrobiologia*, *471*, 101–110.

Bard, E., Arnold, M., Fairbanks, R. G., & Hamelin, B. (1993). ^{230}Th-^{234}U and ^{14}C ages obtained by mass spectrometry on corals. *Radiocarbon*, *35*, 191–199.

Bard, E., Fairbanks, R. G., Hamelin, B., Zindler, A., & Chi Trach, H. (1991). Uranium-234 anomalies in corals older than 150000 years. *Geochimica et Cosmochimica Acta*, *55*, 2385–2390.

Barnes, D. J. (1970). Coral skeletons: An explanation of their growth and structure. *Science*, *170*, 1305–1308.

Beuck, L., & Freiwald, A. (2005). Bioerosion patterns in a deep-water Lophelia pertusa thicket (Propeller Mound, northern Porcupine Seabight). In: A. Freiwald & J. M. Roberts (Eds), *Cold-water corals and ecosystems* (pp. 915–936). Berlin: Springer.

Boerboom, C. M., Smith, J. E., & Risk, M. J. (1998). Bioerosion and micritisation in the deep-sea coral *Desmophyllum cristagalli*. *History of Biology*, *13*, 53–60.

Bond, Z. A., Cohen, A. L., Smith, S. R., & Jenkins, W. J. (2005). Growth and composition of high-Mg calcite in the skeleton of a Bermudian gorgonian (*Plexaurella dichotoma*): Potential for paleo-thermometry. *Geochemistry, Geophysics, Geosystems*, *6*, Q08010, doi:10.1029/2005GC000911.

Broecker, W. S., Gerard, R., Ewing, M., & Heezen, B. C. (1960). Natural radiocarbon in the Atlantic Ocean. *Journal of Geophysical Research*, *65*(a), 2903–2931.

Broecker, W. S., Klas, M., Clark, E., Trumbore, S., Bonani, G., Wolfli, W., & Ivy, S. (1990). Accelerator mass spectrometric measurements on foraminifera shells from deep sea cores. *Radiocarbon*, *32*, 119–133.

Bromley, R. G. (2005). Preliminary study of bioerosion in the deep-water coral Lophelia, Pleistocene, Rhodes, Greece. In: A. Freiwald & J. M. Roberts (Eds), *Cold-water Corals and Ecosystems* (pp. 895–914). Berlin: Springer.

Bryan, W. B., & Hill, D. (1941). Spherulitic crystallization as a mechanism of skeletal growth in the hexacorals. *Proceedings of Royal Society of Queensland*, *52*, 78–91.

Cairns, S. D. (l981). Marine flora and fauna of the northeastern United States. Scleractinia. NOAA Tech. Rept. NMFS Circ. 438: l4pp., l6 figs.

Campana, S. E. (1997). Use of radiocarbon from nuclear fallout as a dated marker in the otoliths of haddock *Melanogrammus aeglefinus*. *Marine Ecology Progress Series*, *150*, 49–56.

Carriquiry, J. D., & Risk, M. J. (1988). Timing and temperature record from stable isotopes of the 1982–1983 El Niño warming event in Eastern Pacific corals. *Palaios*, *3*, 359–364.

Cheng, H., Adkins, J. A., Edwards, R. L., & Boyle, E. A. (2000). U-Th dating of deep-sea corals. *Geochimica et Cosmochimica Acta*, *64*, 2401–2416.

Cline, J. D., & Kaplan, I. R. (1975). Isotopic fractionation of dissolved nitrate during denitrification in the eastern tropical north Pacific Ocean. *Marine Chemistry*, *3*, 271–299.

Cohen, A. L., Lundälv, T., Thorrold, S. R., Corliss, B. H., Smith, S. R., & George, R. Y. (submitted) Sr/Ca variability in the skeleton of a cold-water scleractinian, *Lophelia pertusa*. *Geochemistry, Geophysics, Geosystems*.

QA :5

Cohen, A. L., & McConnaughey, T. A. (2003). Geochemical perspectives on coral mineralization. *Reviews in Mineralogy and Geochemistry*, *54*, 151–187.

Constanz, B. R. (1986). Coral skeleton construction: A physiochemically dominated process. *Palaois*, *1*, 152–157.

Cuif, J.-P., & Dauphin, Y. (2005). The two-step mode of growth in the scleractinian coral skeletons from the microscale to the overall scale. *Journal of Structural Biology*, *150*, 319–331.

DeNiro, M. J., & Epstein, S. (1978). Influence of diet on the distribution of carbon isotopes in animals. *Geochimica et Cosmochimica Acta*, *42*, 495–506.

DeNiro, M. J., & Epstein, S. (1981). Influence of diet on the distribution of nitrogen isotopes in animals. *Geochimica et Cosmochimica Acta*, *45*, 341–351.

Druffel, E. R. M., Griffin, S., Witter, A., Nelson, E., Southon, J., Kashgarian, M., & Vogel, J. (1995). *Gerardia*: Bristlecone pine of the deep-sea? *Geochimica et Cosmochimica Acta*, *59*, 5031–5036.

Druffel, E. R. M., King, L. L., Belastock, R. A., & Buesseler, K. O. (1990). Growth rate of a deep-sea coral using ^{210}Pb and other isotopes. *Geochimica et Cosmochimica Acta*, *54*, 1493–1500.

Edwards, R. L., Beck, W. J., Burr, G. S., Donahue, D. J., Chappell, J. M. A., Bloom, A. L., Druffel, E. R. M., & Taylor, F. W. (1993). A large drop in atmospheric ^{14}C/^{12}C and reduced melting in the Younger Dryas, documented with ^{230}Th ages of corals. *Science*, *260*, 962–967.

Edwards, R. L., Gallup, C. D., & Cheng, H. (2003). Uranium-series dating of marine and lacustrine carbonates. *Reviews in Mineralogy and Geochemistry*, *52*, 363–405.

Emiliani, C., Hudson, J. H., Shinn, E. A., George, R. Y., & Lidz, B. (1978). Oxygen and carbon isotopic growth record in a reef coral from the Florida Keys and a deep-sea coral from Blake Plateau. *Science*, *202*, 627–629.

Epstein, S., Buchsbaum, R., Lowenstam, H. A., & Urey, H. C. (1953). Revised carbonate-water isotopic temperature scale. *Bulletin of the Geological Society of America*, *64*, 1315–1325.

Fallon, S. J., Roark, E. B., Guilderson, T. P., Dunbar, R. B., & Weber, P. (2005). Elemental imaging and proxy development in the deep sea coral, *Corallium secundrum*. Proceedings of 3rd International Symposium on Deep-Sea Corals (p. 187). Miami, USA.

Fallon, S. J., White, J. C., & McCulloch, M. T. (2002). Porites corals as recorders of mining and environmental impacts: Misima Island, Papua New Guinea. *Geochimica et Cosmochimica Acta*, *66*, 45–62.

Frank, N., Lutringer, A., Paterne, M., Blamart, D., Henriet, J. P., van Rooij, D., & van Weering, T. C. E. (2005). Deep-water corals of the northeastern Atlantic margin: Carbonate mound evolution and upper intermediate water ventilation during the Holocene. In: A. Freiwald & J. M. Roberts (Eds), *Cold-Water Corals and Ecosystems* (pp. 113–133). Berlin: Springer.

Frank, N., Paterne, M., Ayliffe, L., van Weering, T., Henriet, J.-P., & Blamart, D. (2004). Eastern North Atlantic deep-sea corals: Tracing upper intermediate water $\Delta^{14}C$ during the Holocene. *Earth and Planetary Science Letters*, *219*, 297–309.

Fry, B., & Sherr, E. B. (1984). $\delta^{13}C$ measurements as indicators of carbon flow in marine and freshwater ecosystems. *Contributions in Marine Science*, *27*, 13–47.

Furla, P., Bénazet-Tambutté, S., Jaubert, J., & Allemand, D. (1998). Diffusional permeability of dissolved inorganic carbon through the isolated oral epithelial layers of the sea anemone, *Anemonia viridis*. *Journal of Experimental Marine Biology and Ecology*, *230*, 71–88.

Gagnon, A. C., & Adkins, J. F. (2005). *Multiple proxy "vital effects" in a deep-sea coral*. Proceedings of 3rd International Symposium on Deep-Sea Corals (p. 188). Miami, USA.

Ganeshram, R. S., Pederson, T. F., Calvert, S. E., & Murray, J. W. (1995). Large changes in oceanic nutrient inventories from glacial to interglacial periods. *Nature*, *376*, 755–757.

Gladfelter, E. H. (1982). Skeletal development in *Acropora cervicornis*: I. Patterns of calcium carbonate accretion in the axial corallite. *Coral Reefs*, *1*, 45–51.

Goldberg, W. M. (1991). Chemistry and structure of skeletal growth rings in the black coral Antipathes fiordenis (Cnidaria, Antipatharia). *Hydrobiologia*, *217/216*, 403–409.

Goldstein, S. J., Lea, D. W., Chakraborty, S., Kashgarian, M., & Murrell, M. T. (2001). Uranium-series and radiocarbon geochronology of deep-sea corals: Implications for Southern Ocean ventilation rates and the oceanic carbon cycle. *Earth and Planetary Science Letters*, *193*, 167–182.

Goodfriend, G. A. (1997). Aspartic acid racemization and amino acid composition of the organic endoskeleton of the deep-water colonial anemone *Gerardia*: Determination of longevity from kinetic experiments. *Geochimica et Cosmochimica Acta*, *61*, 1931–1939.

Goreau, T. F. (1959). The physiology of skeletal formation in corals I. A method for measuring the rate of calcium deposition by corals under different conditions. *Biological Bulletin*, *116*, 59–75.

Grasshoff, M., & Zibrowius, H. (1983). Kalkkrusten auf Achsen von Hornkorallen. *Senckenbergiana Maritima*, *15*, 111–145.

Griffin, S., & Druffel, E. R. M. (1989). Sources of carbon to deep-sea corals. *Radiocarbon*, *31*, 533–543.

Grossman, E. L., & Ku, T.-L. (1986). Oxygen and carbon isotope fractionation in biogenic aragonite: Temperature effects. *Chemical Geology (Isotope Geoscience Section)*, *59*, 59–74.

Haug, G. H., Pederson, T. F., Sigman, D. M., Calvert, S. E., Nielsen, B., & Peterson, L. C. (1998). Glacial/interglacial variations in production and nitrogen fixation in the Cariaco Basin during the last 580 kyr. *Paleoceanography*, *13*, 427–432.

Heikoop, J. M., Hickmott, D. D., Risk, M. J., Shearer, C. K., & Atudorei, V. (2002). Potential climate signals from the deep-sea gorgonian coral *Primnoa resedaeformis*. *Hydrobiologia*, *471*, 117–124.

Heikoop, J. M., Risk, M. J., Lazier, A. V., & Schwarcz, H. P. (1998). $\delta^{18}O$ and $\delta^{13}C$ signatures of a deep-sea gorgonian coral from the Atlantic coast of Canada. *EOS*, *79*(17, supplement), S179.

Heikoop, J. M., Tsujita, C. J., & Risk, M. J. (1996). Corals as proxy recorders of volcanic activity: Banda Api, Indonesia. *Palaois*, *11*, 286–292.

Henderson, G. M. (2002). Seawater ($^{234}U/^{238}U$) during the last 800 thousand years. *Earth and Planetary Science Letters*, *199*, 97–110.

Hendy, E. J., Gagan, M. K., Alibert, C. A., McCulloch, M. T., Lough, J. M., & Isdale, P. J. (2002). Abrupt decrease in tropical Pacific sea surface salinity at end of Little Ice Age. *Science*, *295*, 1511–1514.

Jasper, J. P., Hayes, J. M., Mix, A. C., & Prahl, F. G. (1994). Photosynthetic fractionation of ^{13}C and concentrations of dissolved CO_2 in the central equatorial Pacific during the last 255,000 years. *Paleoceanography*, *9*, 781–798.

Johnston, I. S. (1980). The ultrastructure of skeletogenesis in hermatypic corals. *International Review of Cytology*, *67*, 171–214.

Key, R. M. (2001). Radiocarbon. In: J. Steele, S. Thorpe & K. Turekian (Eds), *Encyclopedia of Ocean Sciences* (pp. 2338–2353). London: Academic Press.

Knapp, A. N., Sigman, D. M., & Lipschultz, F. (2005). N isotopic composition of dissolved organic nitrogen and nitrate at the Bermuda Atlantic time-series site. *Global Biogeochemical Cycles*, *19*, GB1018, doi:10.1029/2004GB002320.

Kroopnick, P. (1985). The distribution of ^{13}C of $\sum CO_2$ in the world oceans. *Deep-Sea Research I*, *32*, 57–84.

Laws, E. A., Popp, B. N., Cassar, N., & Tanimoto, J. (2002). ^{13}C discrimination patterns in oceanic phytoplankton: Likely influence of CO_2 concentrating mechanisms, and implications for palaeoreconstructions. *Functional Plant Biology*, *29*, 323–333.

Lazier, A. V., Smith, J. E., & Risk, M. J. (1999). The skeletal structure of *Desmophyllum cristagalli*: The use of deep-water corals in sclerochronology. *Lethaia*, *32*, 119–130.

Lewis, J. C., Barnowski, T. F., & Telesnicki, G. J. (1992). Characteristics of carbonates of gorgonian axes. *Biological Bulletin*, *183*, 278–296.

Lomitschka, M., & Mangini, A. (1999). Precise Th/U-dating of small and heavily coated samples of deep sea corals. *Earth and Planetary Science Letters*, *170*, 391–401.

Ludwig, K. R., & Titterington, D. M. (1994). Calculation of $^{230}Th/U$ isochrons, ages and errors. *Geochimica et Cosmochimica Acta*, *58*, 5031–5042.

Lutringer, A., Blamart, D., Frank, N., & Labeyrie, L. (2005). Paleotemperatures from deep-sea corals scale effects. In: A. Freiwald & J. M. Roberts (Eds), *Cold-Water Corals and Ecosystems* (pp. 1081–1096). Berlin: Springer.

Macintyre, I. G., Bayer, F. M., Logan, M. A., & Skinner, H. C. W. (2000). Possible vestige of early phosphatic biomineralization in gorgonian octocorals (Coelenterata). *Geology*, *28*, 455–458.

Mangini, A., Lomitschka, M., Eichstadter, R., Frank, N., & Vogler, S. (1998). Coral provides way to age deep water. *Nature*, *392*, 347–348.

Marschal, C., Garrabou, J., Harmelin, J. G., & Pichon, M. (2004). A new method for measuring growth and age in the precious red coral *Corallium rubrum* (L.). *Coral Reefs*, *23*, 423–432.

McClelland, J. W., & Montoya, J. P. (2002). Trophic relationships and the nitrogen isotopic composition of amino acids in plankton. *Ecology*, *83*, 2173–2180.

McConnaughey, T. A. (1989a). ^{13}C and ^{18}O isotope disequilibria in biological carbonates. 1. Patterns. *Geochimica et Cosmochimica Acta*, *53*, 151–162.

McConnaughey, T. A. (1989b). ^{13}C and ^{18}O isotope disequilibria in biological carbonates. 2. *In vitro* simulation of kinetic isotope effects. *Geochimica et Cosmochimica Acta*, *53*, 163–171.

McConnughey, T. A. (2003). Sub-equilibrium oxygen-18 and carbon-13 levels in biological carbonates: carbonate and kinetic models. *Coral Reefs*, *22*, 316–327.

Montagna, P., McCulloch, M., Taviani, M., Remia, A., & Rouse, G. (2005). High-resolution trace element compositions in deep-water scleractinian corals (*Desmophyllum dianthus*) from the Mediterranean Sea and the Great Australian Bight. In: A. Freiwald & J. M. Roberts (Eds), *Cold-Water Corals and Ecosystems* (pp. 1109–1126). Berlin: Springer.

Mortensen, P. B., & Rapp, H. T. (1998). Oxygen and carbon isotope ratios related to growth line patterns in skeletons of Lophelia pertusa (L.) (Anthozoa, Sclleractinia): Implications for determination of linear extension rates. *Sarsia*, *83*, 433–446.

Orejas, C., Gili, J. M., & Arntz, W. (2003). Role of small-plankton communities in the diet of two Antarctic octocorals (*Primnoisis antarctica* and *Primnoella* sp.). *Marine Ecology Progress Series*, *250*, 105–116.

Pons-Branchu, E., Hillaire-Marcel, C., Deschamps, P., Ghaleb, B., & Sinclair, D. J. (2005). Early diagenesis impact on precise U-series dating of deep-sea corals: Example of a 100–200-year old *Lophelia pertusa* sample from the northeast Atlantic. *Geochimica et Cosmochimica Acta*, *69*, 4865–4879.

Rau, G. H. (1994). Variations in sedimentary organic $\delta^{13}C$ as a proxy for past changes in ocean and atmospheric [CO_2]. In: R. Zahn, M. Kamiski, L. D. Labeyrie & T. F. Pedersen (Eds), *Carbon Cycling in the Glacial Ocean Constraints on the Ocean's Role in Global Climate Change* (pp. 307–322). Berlin: Springer.

Remia, A., & Taviani, M. (2004). Shallow-buried Pleistocene Madrepora-coral mounds on a muddy continental slope. Tuscan Archipelago, NE Tyrrhenian Sea. Facies 50. doi:10.1007/s10347-004-0029-2.

Ribes, M., Coma, R., & Gili, J. M. (1999). Heterogeneous feeding in benthic suspension feeders: The natural diet and grazing rate of the temperate gorgonian *Paramuricea clavata* (Cnidaria: Octocorallia) over a year cycle. *Marine Ecology Progress Series*, *183*, 125–137.

Ribes, M., Coma, R., & Rossi, S. (2003). Natural feeding of the temperate asymbiotic octocoral-gorgonian *Leptogorgia sarmentosa* (Cnidaria: Octocorallia). *Marine Ecology Progress Series*, *254*, 141–150.

Risk, M. J., Hall-Spenser, J., & Williams, B. (2005). Climate records from the Faroe-Shetland Channel using *Lophelia pertusa* (Linnaeus, 1758). In: A. Freiwald & J. M. Roberts (Eds), *Cold-water corals and ecosystems* (pp. 1097–1108). Berlin: Springer.

Risk, M. J., Heikoop, J. M., Snow, M. G., & Beukens, R. (2002). Lifespans and growth patterns of two deep-sea corals: *Primnoa resedaeformis* and *Desmophyllum cristagalli*. *Hydrobiologia*, *471*, 125–131.

Roark, E. B., Guilderson, T. P., Flood-Page, S., Dunbar, R. B., Ingram, B. L., Fallon, S. J., & McCulloch, M. (2005). Radiocarbon-based ages and growth rates of bamboo corals from the Gulf of Alaska. *Geophysical Research Letters*, *32*, L04606, doi:10.1029/2004GL021919.

Robinson, L. F., Adkins, J. F., Fernandez, D. P., Burnett, D. S., Wang, S.-L., Gagnon, A. C., & Krakauer, N. (2006). Primary U distribution in scleractinian corals and its implications for U series dating. *Geochemistry, Geophysics, Geosystems*, 7, Q05022.

Robinson, L. F., Adkins, J. F., Keigwin, L. D., Southon, J., Fernandez, D. P., Wang, S.-L., & Scheirer, D. S. (2005). Radiocarbon variability in the Western North Atlantic during the Holocene. *Science*, *310*, 1469–1473.

Rollion-Bard, C., Blamart, D., & Cuif, J.-P. (2003). Microanalysis of C and O isotopes of azooxanthellate and zooxanthellate corals by ion microprobe. *Coral Reefs*, *22*, 405–415.

Saino, T., & Hattori, A. (1987). Geographical variation in the water column distribution of suspended particulate organic nitrogen and its ^{15}N natural abundance in the Pacific and its marginal seas. *Deep-Sea Research A*, *34*, 807–827.

Sarnthein, M., Winn, K., Jung, S. J. A., Duplessy, J.-C., Labeyrie, L., Erlenkeuser, H., & Ganssen, G. (1994). Changes in east Atlantic deepwater circulation over the last 30,000 years: Eight time slice reconstructions. *Paleoceanography*, *9*, 209–267.

Schröder-Ritzrau, A., Freiwald, A., & Mangini, A. (2005). U/Th-dating of deep-water corals from the eastern North Atlantic and the weatern Mediterranean Sea. In: A. Freiwald & J. M. Roberts (Eds), *Cold-Water Corals and Ecosystems* (pp. 157–172). Berlin: Springer.

Schröder-Ritzrau, A., Mangini, A., & Lomitschka, M. (2003). Deep-sea corals evidence periodic reduced ventilation in the North Atlantic during the LGM/Holocene transition. *Earth and Planetary Science Letters*, *216*, 399–410.

Shackleton, N. J. (1967). Oxygen isotope analyses and Pleistocene temperatures reassessed. *Nature*, *215*, 15–17.

Shen, G. T., & Boyle, E. A. (1988). Determination of lead, cadmium, and other trace metals in annually-banded corals. *Chemical Geology*, *67*, 47–62.

Sherwood, O. A. (2002). *The deep-sea gorgonian Primnoa resedaeformis as an oceanographic monitor* (p. 65). M.Sc. Thesis. McMaster University, Hamilton, Canada.

Sherwood, O. A. (2006). *Deep-sea octocorals: Dating methods, stable isotopic composition, and proxy records of the slopewaters off Nova Scotia* (p. 240). Ph.D. Thesis. Dalhousie University, Halifax, Canada.

Sherwood, O. A., Heikoop, J. M., Scott, D. B., Risk, M. J., Guilderson, T. P., & McKinney, R. A. (2005b). Stable isotopic composition of deep-sea gorgonian corals *Primnoa* spp.: A new archive of surface processes. *Marine Ecology Progress Series*, *301*, 135–148.

Sherwood, O. A., Heikoop, J. M., Sinclair, D. J., Scott, D. B., Risk, M. J., Shearer, C., & Azetsu-Scott, K. (2005c). Skeletal Mg/Ca in Primnoa resedaeformis: Relationship to temperature? In: A. Freiwald & J. M. Roberts (Eds), *Cold-water corals and ecosystems* (pp. 1061–1079). Berlin: Springer.

Sherwood, O. A., Scott, D. B., & Risk, M. J. (2006). Late Holocene radiocarbon and aspartic acid racemization dating of deep-sea octocorals. *Geochimica et Cosmochimica Acta*, *70*, 2806–2814.

Sherwood, O. A., Scott, D. B., Risk, M. J., & Guilderson, T. P. (2005a). Radiocarbon evidence for annual growth rings in the deep-sea octocoral *Primnoa resedaeformis*. *Marine Ecology Progress Series*, *301*, 129–134.

Shirai, K., Kusakabe, M., Nakai, S., Ishii, T., Watanabe, T., Hiyagon, H., & Sano, Y. (2005). Deep-sea coral geochemistry: Implication for the vital effect, 224, 212–222. QA :6

Sigman, D. M., Altabet, M. A., McCorkle, D. C., Francois, R., & Fischer, G. (2000). The δ^{15}N of nitrate in the Southern Ocean: Nitrogen cycling and circulation in the ocean interior. *Journal of Geophysical Research*, *105*(C8), 19599–19614.

Sinclair, D. J. (2005). Correlated trace element "vital effects" in tropical corals: A new geochemical tool for probing biomineralization. *Geochimica et Cosmochimica Acta*, *69*, 3265–3284.

Sinclair, D. J., & Risk, M. J. (in press) A numerical model of trace-element co-precipitation in a physicochemical calcification system: Application to coral biomineralization and trace element 'vital effects'. *Geochimica et Cosmochimica Acta*. QA :7

Sinclair, D. J., Sherwood, O. A., Risk, M. J., Hillaire-Marcel, C., Tubrett, M., Sylvester, P., McCulloch, M., & Kinsley, L. (2005). Testing the reproducibility of Mg/Ca profiles in the deep-water coral *Primnoa resedaeformis*: Putting the proxy through its paces. In: A. Freiwald & J. M. Roberts (Eds), *Cold-water corals and ecosystems* (pp. 1039–1060). Berlin: Springer.

Sinclair, D. J., Williams, B., Risk, M. J., & McCulloch, M. T. (submitted) Trace-element "vital effects"—a ubiquitous feature of scleractinian coral skeletons, Science

Smith, J. E., Risk, M. J., Schwarcz, H. P., & McConnaughey, T. A. (1997). Rapid climate change in the North Atlantic during the Younger Dryas recorded by deep-sea corals. *Nature*, *386*, 818–820.

Smith, J. E., Schwarcz, H. P., & Risk, M. J. (2002). Patterns of isotopic disequilibria in azooxanthellate coral skeletons. *Hydrobiologia*, *471*, 111–115.

Smith, J. E., Schwarcz, H. P., Risk, M. J., McConnaughey, T. A., & Keller, N. (2000). Paleotemperatures from deep-sea corals: Overcoming "vital effects". *Palaios*, *15*, 25–32.

Sorauf, J. E., & Jell, J. S. (1977). Structure and incremental growth in the ahermatypic coral *Desmophyllum cristagalli* from the North Atlantic. *Palaeontology*, *20*, 1–19.

Stuiver, M., Quay, P. D., & Ostlund, H. G. (1983). Abyssal C-14 distribution and the age of the world oceans. *Science*, *219*, 849–851.

Swart, P. K., & Hubbard, J. A. E. B. (1982). Uranium in scleractinian coral skeletons. *Coral Reefs*, *1*, 13–19.

Szmant-Froelich, A. (1974). Structure, iodination, and growth of the axial skeletons of *Muricea californica* and *M. fruticosa* (Coelenterata: Gorgonacea). *Marine Biology*, *27*, 299–306.

Teichert, C. (1958). Cold- and deep-water coral banks. *AAPG Bulletin*, *42*, 1064–1082.

Thresher, R., Rintoul, S. R., Koslow, J. A., Weidman, C., Adkins, J., & Proctor, C. (2004). Oceanic evidence of climate change in southern Australia over the last three centuries. *Geophysical Research Letters*, *31*, L07212, doi:10.1029/2003GL018869.

Thunell, R. C., Sigman, D. M., Muller-Karger, F., Astor, Y., & Varela, R. (2004). Nitrogen isotope dynamics of the Cariaco Basin, Venezuela. *Global Biogeochemical Cycles*, *18*, GB3001, doi:10.1029/2003GB002185.

Titschak, J., & Freiwald, A. (2005). Growth, deposition and faciesof Pleistocene bathyal coral communities from Rhodes, Greece. In: A. Freiwald & J. M. Roberts (Eds), *Cold-Water Corals and Ecosystems* (pp. 41–59). Berlin: Springer.

Tudhope, A. W., Chilcott, C. P., McCulloch, M. T., Cook, E. R., Chappell, J., Ellam, R. M., Lea, D. W., Lough, J. M., & Shimmield, G. B. (2001). Variability in the El Niño-Southern oscillation through a glacial-interglacial cycle. *Science*, *291*, 1511–1517.

Wainwright, S. (1964). Studies of the mineral phase of coral skeleton. *Experimental Cell Research*, *34*, 213–230.

Ward-Paige, C. A., Risk, M. J., & Sherwood, O. A. (2005). Reconstruction of nitrogen sources on coral reefs: δ^{15}N and δ^{13}C in gorgonians from the Florida Reef Tract. *Marine Ecology Progress Series*, *296*, 155–163.

Weber, J. N. (1973). Deep-sea scleractinian coral: Isotopic composition of skeleton. *Deep Sea Research*, *2*, 901–909.

Weinbauer, M. G., Brandstätter, F., & Velimirov, B. (2000). On the potential use of magnesium and strontium concentrations as ecological indicators in the calcite skeleton of the red coral (*Corallium rubrum*). *Marine Biology*, *137*, 801–809.

Williams, B., Risk M. J., Sulak, K., Ross, S., & Stone, R. (2005). Deep-water Antipatharians and Gorgonians: Proxies of biogeochemical processes. *Proceedings of 3rd International Symposium on Deep-Sea Corals* (p. 70). Miami, USA.

Wisshak, M., Freiwald, A., Lundälv, T., & Gektidis, M. (2005). The physical niche of the bathyal *Lophelia pertusa* in a non-bathyal setting: environmental controls and paleoecological implications. In: A. Freiwald & J. M. Roberts (Eds), *Cold-Water Corals and Ecosystems* (pp. 979–1001). Berlin: Springer.

Wu, J., Calvert, S. E., & Wong, C. S. (1999). Carbon and nitrogen isotope ratios in sedimenting particulate organic matter at an upwelling site off Vancouver Island. *Estuarine Coastal and Shelf Science*, *48*, 193–203.